ISSN 0083-7903, 73 (Print)
ISSN 2538-1016; 73 (Online)

Hydrology of the Kermadec Islands Region

by

N.M. RIDGWAY and R.A. HEATH

New Zealand Oceanographic Institute Memoir 73

1975

NEW ZEALAND

DEPARTMENT OF SCIENTIFIC AND INDUSTRIAL RESEARCH

Hydrology of the Kermadec Islands Region

by

N.M. RIDGWAY and R.A. HEATH

New Zealand Oceanographic Institute, Wellington

New Zealand Oceanographic Institute Memoir 73

1975

Citation according to "World List of Scientific Periodicals" (4th edn)

Mem. N.Z. oceanogr. Inst. 73

ISSN 0083 - 7903

Received for publication : February 1972

A.R. SHEARER, GOVERNMENT PRINTER, WELLINGTON, NEW ZEALAND - 1975

CONTENTS

Abstract 5
Introduction 5
Data presentation 6
Discussion 8
Geostrophic circulation 8
Surface temperature and surface salinity 9
Upper mixed layers 10
Temperature and salinity at 200 m depth 11
Antarctic Intermediate Water 19
Vertical profiles of temperature and salinity 19
Sound velocity 19
Conclusion 21
Acknowledgments 21
References 21
Appendix - Numerical station data 23

FIGURES

1. Station positions and the bathymetry of the survey area. 6
2. Geopotential topography of the sea surface relative to 1 000 dbars. 8
3. Geopotential topography of the sea surface relative to 500 dbars and of the 500 dbar surface relative to 1 000 dbars. 9
4. Distribution of surface isotherms. 10
5. Distribution of surface isohalines. 11
6. Isobaths of the depth of the upper mixed layer. 12
7. Bathythermograph traces. .. .. .. 13 & 14
8. Distribution of isotherms at a depth of 200 m 15
9. Distribution of isohalines at a depth of 200 m. 16
10. Distribution of isohalines of minimum salinity. 17
11. Isobaths of the depth of the minimum salinity. 18
12. Vertical meridional cross section of temperature and salinity. .. 19
13. Vertical zonal cross section of temperature and salinity. .. 20
14. Vertical meridional cross section of sound velocity. 21

TABLES

1. Station circumstances. 7
2. Wind stresses in 5° square northeast of New Zealand, December-February as given by Hidaka (1958). 16

Hydrology of the Kermadec Islands Region

by

N.M Ridgway and R.A. Heath

ABSTRACT

The results of a hydrological survey made in an area lying to the north-east of New Zealand are presented and analysed. A total of 33 serial temperature-salinity stations was occupied to a maximum depth of 2500 m and the survey, conducted in February-March 1968, was the sixth of a series carried out in the ocean around New Zealand in consecutive summers. Geostrophic flow in the area is discussed and the effect of wind stress upon this flow is considered. Sound velocities are calculated from the observed data and velocity corrections for echo sounding machines are derived for the area surveyed.

INTRODUCTION

Between 20 February and 10 March 1968, 33 hydrological stations were occupied within the region bounded by latitudes 28°S and 35°S and longitudes 175°E and 175°W. In this region the north-south oriented Kermadec and Colville Ridges are separated by the Havre Trough. The deep Kermadec Trench is located east of the Kermadec Ridge and the South Fiji Basin is located west of the Colville Ridge. These features, together with the station positions, are shown in Fig. 1.

This survey was the sixth of a series conducted in successive summers in different areas around New Zealand from N.Z. Oceanographic Institute's research vessel, MV *Taranui*. The results of previous surveys have been presented by Garner (1967a, 1967b, 1970) and Ridgway (1970).

At each station, temperatures and pressures were measured with Negretti and Zambra reversing thermometers, mounted on Knudsen reversing bottles. A bathythermograph was also used to define the temperature/depth relationships in the upper 270 m of the water. The observed readings of the protected and unprotected thermometers were corrected and thermometric depths obtained from these readings by using the Culbertson slide rule (Culbertson 1955) and thermometer calibration certificates provided by National Physical Laboratory, England. The consistency of the results obtained was verified by plots using the procedure described by LaFond (1951). Temperature, salinity and depth-dependent quantities were computed on an Elliott 503 computer using formulae given by LaFond (1951, p. 14) for density and dynamic height and by Wilson (1960) for

New Zealand Oceanographic Institute Memoir 73. 1975. 28 p.
ISSN 0083 - 7903

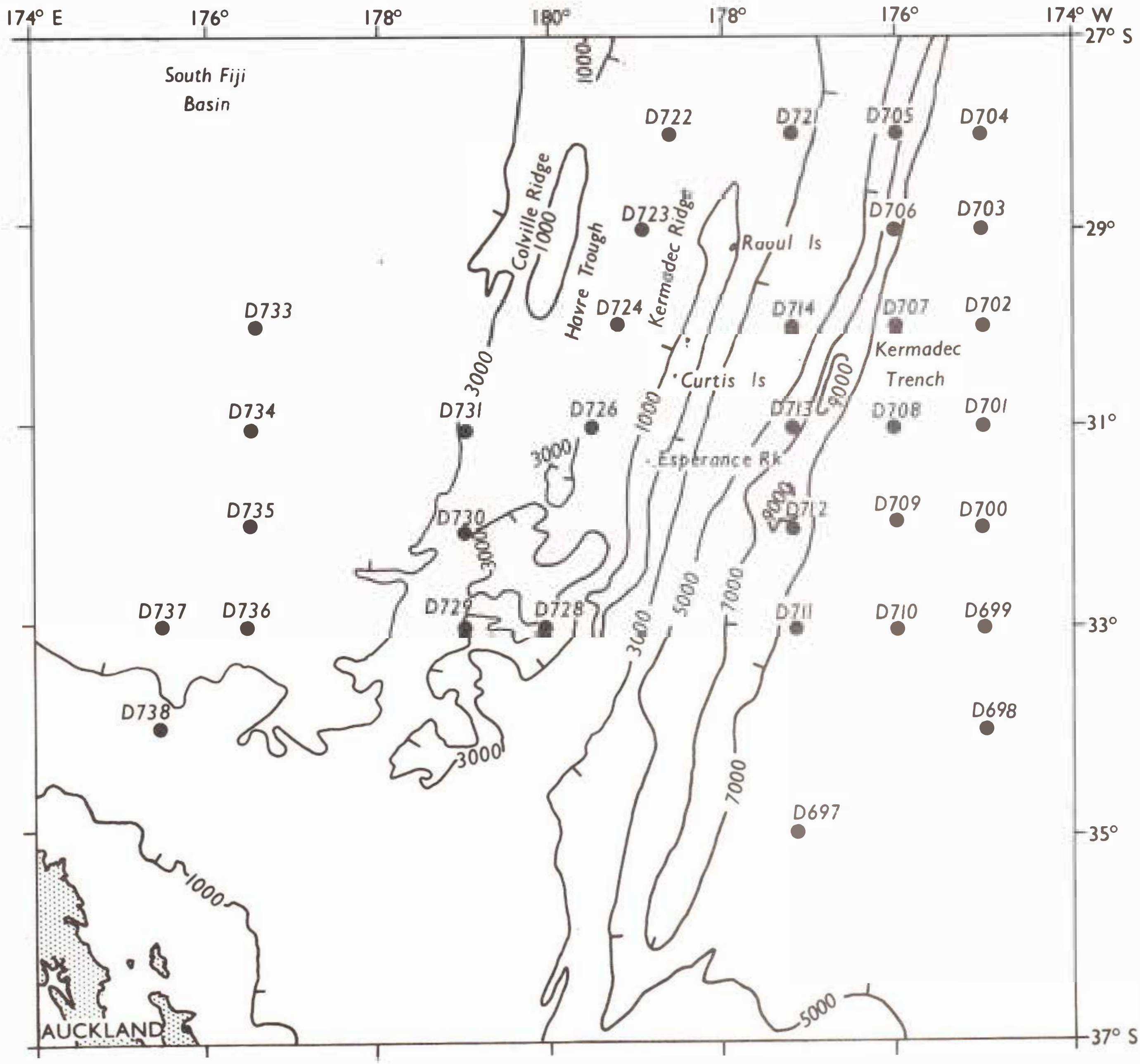

Fig. 1. Station positions and the bathymetry of the survey area. Depths are in metres.

sound velocity. The mean vertical sounding velocity was computed by numerical integration of the sound velocity-depth relationship.

Conductivities of the water samples were determined by an inductively-coupled salinometer (Brown and Hamon 1961) standardised against Copenhagen Standard Sea Water, the conductivities being converted to salinities using tables published by the National Institute of Oceanography of Great Britain and UNESCO (1966). Surface temperature was recorded throughout the cruise by a thermograph whose sensing element was located in the ship's sea water inlet pipe.

Station circumstances are given in Table 1.

Data Presentation

Observed values of temperature and salinity at the depths of sampling together with the computed values of density, sound velocity and dynamic height anomaly are listed in the Appendix.

Distributions of various properties are illustrated in the figures and reference to these is made in the following discussion.

TABLE 1

STATION CIRCUMSTANCES

Air (screen) temperature and wind properties estimated at bridge level.

Station No.	N.Z. Date / Time		Depth (m)	Air Temp. (°C)	Wind		Latitude (South)	Longitude (West unless otherwise indicated)
	Start	Finish			Dirn (°T)	Speed (ms^{-1})		
	February / March 1968							
D697	20/0653	20/0930	5700	19.5	340	6	35°00'	177°00'
D698	21/0608	21/0902	5700	21.5	240	5	34°00'	175°00'
D699	21/1538	21/1840	5020	21.3	230	3	33°00'	175°00'
D700	22/0115	22/0403	5700	21.5	220	3	32°00'	175°00'
D701	22/1239	22/1512	4898	22.8	140	7	31°00'	175°00'
D702	22/2200	23/0014	5670	22.2	150	5	30°00'	175°00'
D703	23/0722	23/1025	5750	22.5	140	8	29°00'	175°00'
D704	23/1657	23/1957	6200	23.0	130	7	28°00'	175°00'
D705	24/0650	24/1105	6500	23.0	110	7	28°00'	176°00'
D706	25/0145	25/0412	9000	22.4	120	7	29°00'	176°00'
D707	25/1301	25/1619	6750	22.6	120	7	30°00'	176°00'
D708	26/0026	26/0221	5700	22.9	120	4	31°00'	176°00'
D709	26/0950	26/1145	5700	22.5	160	5	31°56.5'	176°00'
D710	26/1924	26/2152	6100	21.0	140	2	33°00'	176°00'
D711	27/0439	27/0639	6600	20.8	290	1	33°00'	177°10'
D712	27/1300	27/1453	9053	23.1	090	3	32°00'	177°10'
D713	27/2141	27/2310	7000	22.0	100	4	31°00'	177°10'
D714	28/0652	28/0850	5100	22.5	090	6	30°00'	177°10'
D721	1/1606	1/1830	2377	24.0	100	12	28°00'	177°00'
D722	2/0447	2/0726	2487	23.4	120	12	27°59'	178°38'
D723	2/1631	2/1846	2560	23.0	110	15	29°00'	178°55'
D724	3/0320	3/0604	2496	21.6	110	10	29°55'	179°15'
D726	3/2212	4/0210	2475	22.4	100	7	31°00'	179°30'
D728	4/2130	4/2340	3000	21.8	090	9	33°00'	180°00'
D729	5/0509	5/0835	3250	21.8	090	13	32°59'	179°05'E
D730	5/1554	5/1830	2750	22.5	080	19	32°04'	178°59'E
D731	6/0616	6/0916	2700	22.2	090	14	31°00'	179°00'E
D733	8/0600	8/0852	4300	25.0	020	7	30°01'	176°40'E
D734	8/1500	8/2113	4100	23.7	050	7	31°00'	176°30'E
D735	9/0600	9/0815	3950	22.6	060	7	32°00'	176°34'E
D736	9/1403	9/1623	3750	23.6	040	5	33°00'	176°30'E
D737	9/2200	9/2350	3750	23.4	010	4	33°00'	175°30'E
D738	10/0616	10/0817	2000	23.8	320	3	34°00'	175°28'E

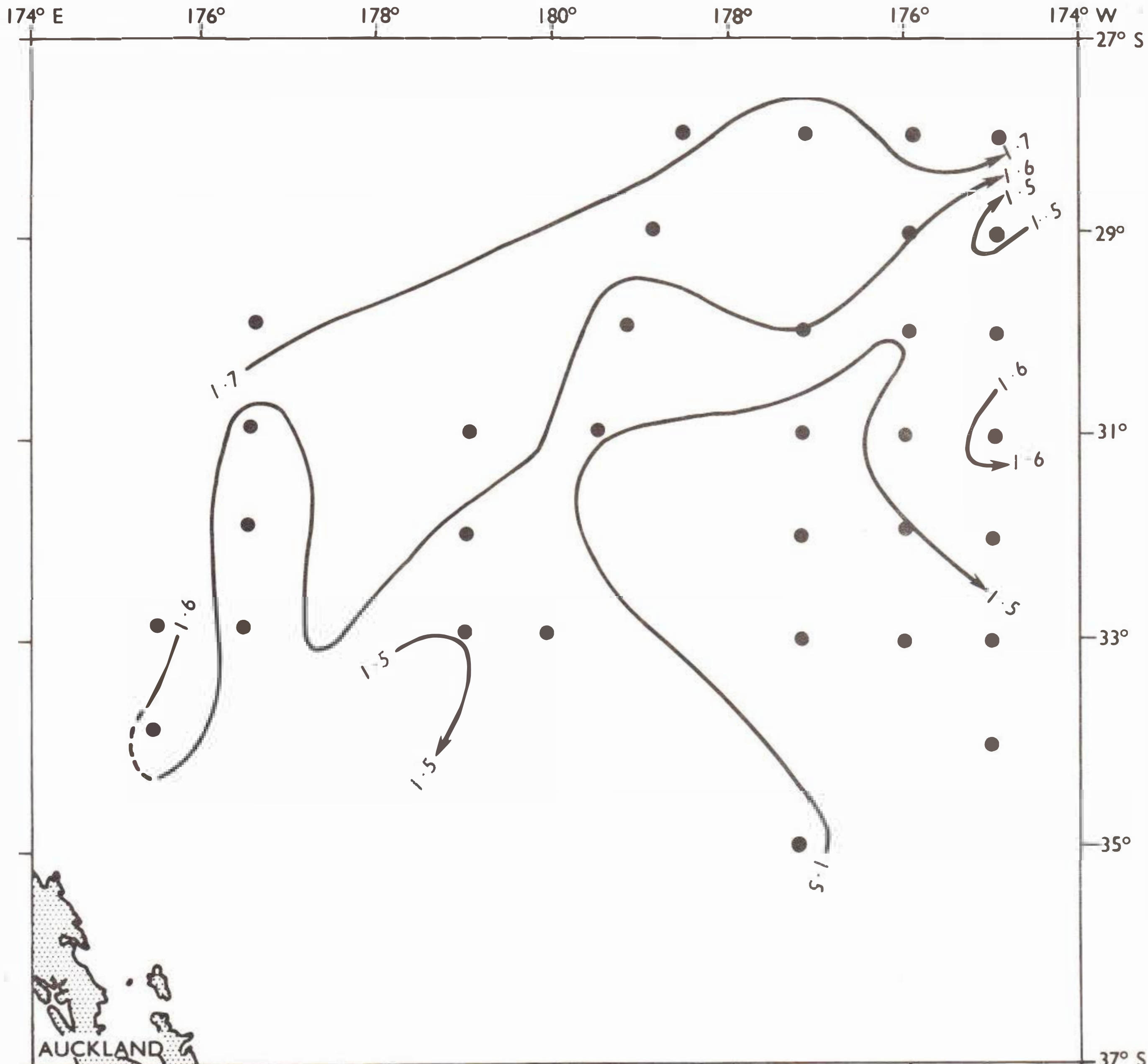

Fig. 2. Geopotential topography of the sea surface relative to 1 000 dbars. Contours (in dynamic metres) represent geostrophic flow in the direction of the arrows.

DISCUSSION

Geostrophic Circulation

The streamlines of surface geostrophic flow with respect to 1000 dbars (Fig. 2), which indicate the surface geostrophic currents relative to a depth of c. 1000 m, were generally from west to east. The surface geostrophic currents with respect to 500 dbars and the geostrophic currents at 500 dbars relative to 1000 dbars (Fig. 3) also flowed from west to east although the 500/1000 dbars current was weaker than the 0/500 dbar current. Since the flow is generally weak, no real significance, other than a general flow towards the east, should be placed on the contours. The limitations of the data are such that the errors in the dynamic height anomalies at any station may be of comparable size to the horizontal differences between adjacent stations. The general geostrophic flow from west to east is in agreement with the geostrophic circulation at the surface relative to 1000 dbars given by Reid (1961) and Wyrtki (1962) and is continuous with the geostrophic circulation shown by Garner (1969) in the area immediately to the west.

The 1.6 and 1.7 dyn. m contours of the surface, relative to 1000 dbars (Fig. 2) are deflected slightly northwards over the Kermadec Ridge and slightly southwards over the Kermadec Trench. Similar deflections are evident in both the 0/500 dbar and 500/1000 dbar dynamic height contours (Fig. 3), the deflections being most prominent in the 500/1000 dbar contours. These deflections are in agreement with a deflection to the right over increasing depths and to the left over decreasing depths in the Southern Hemisphere (*see* e.g. Neumann 1960, p. 133).

Surface Temperature and Surface Salinity

The surface temperature and salinity (Figs 4, 5) ranged from minimum values of 20.5°C and 34.45‰, found at the southernmost station (D697), to maximum

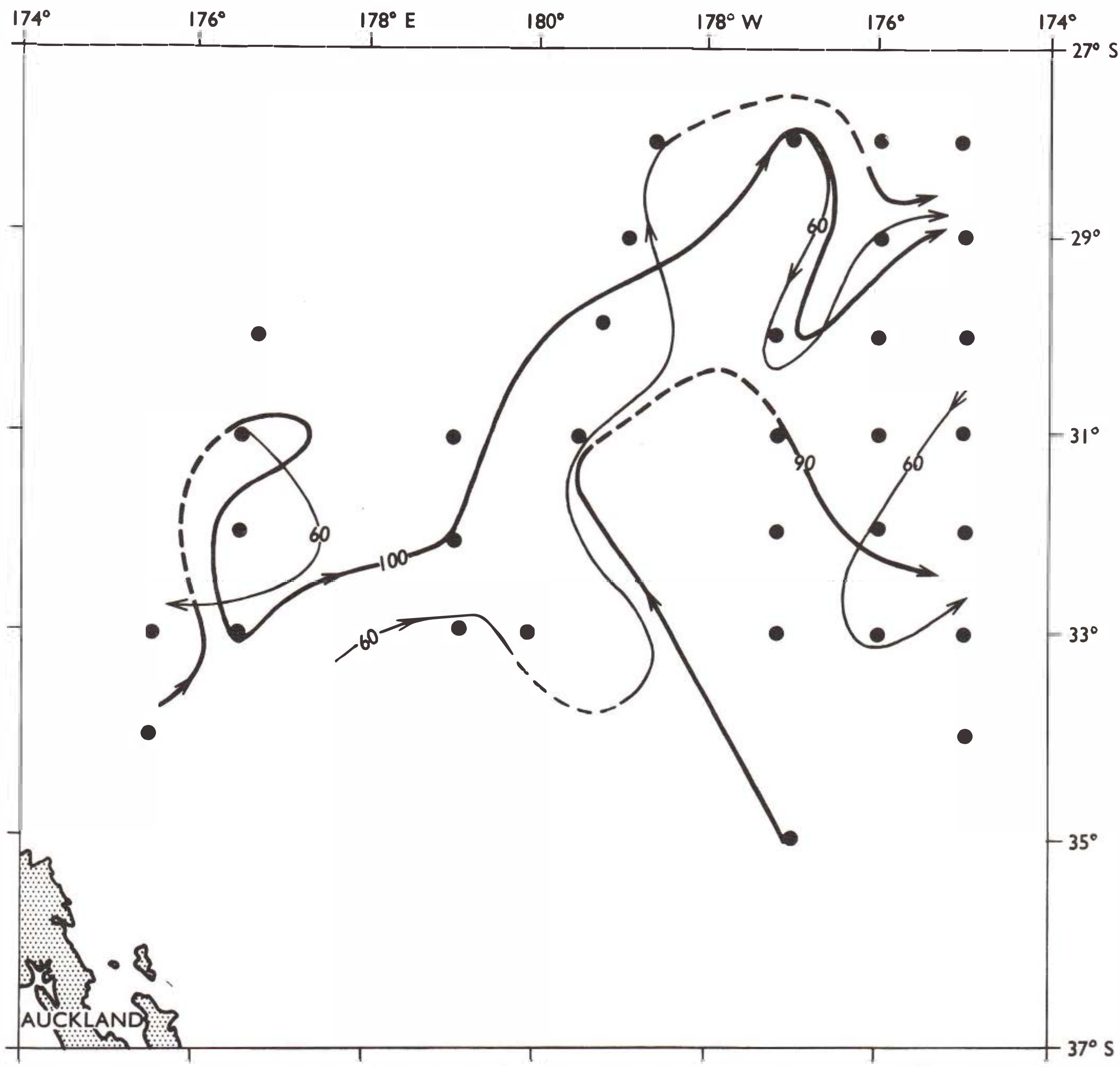

Fig. 3. Geopotential topography of the sea surface relative to 500 dbars (heavy black) and of the 500 dbar surface relative to 1000 dbars (light black). Contours (in dynamic metres) represent geostrophic flow in the direction of the arrows.

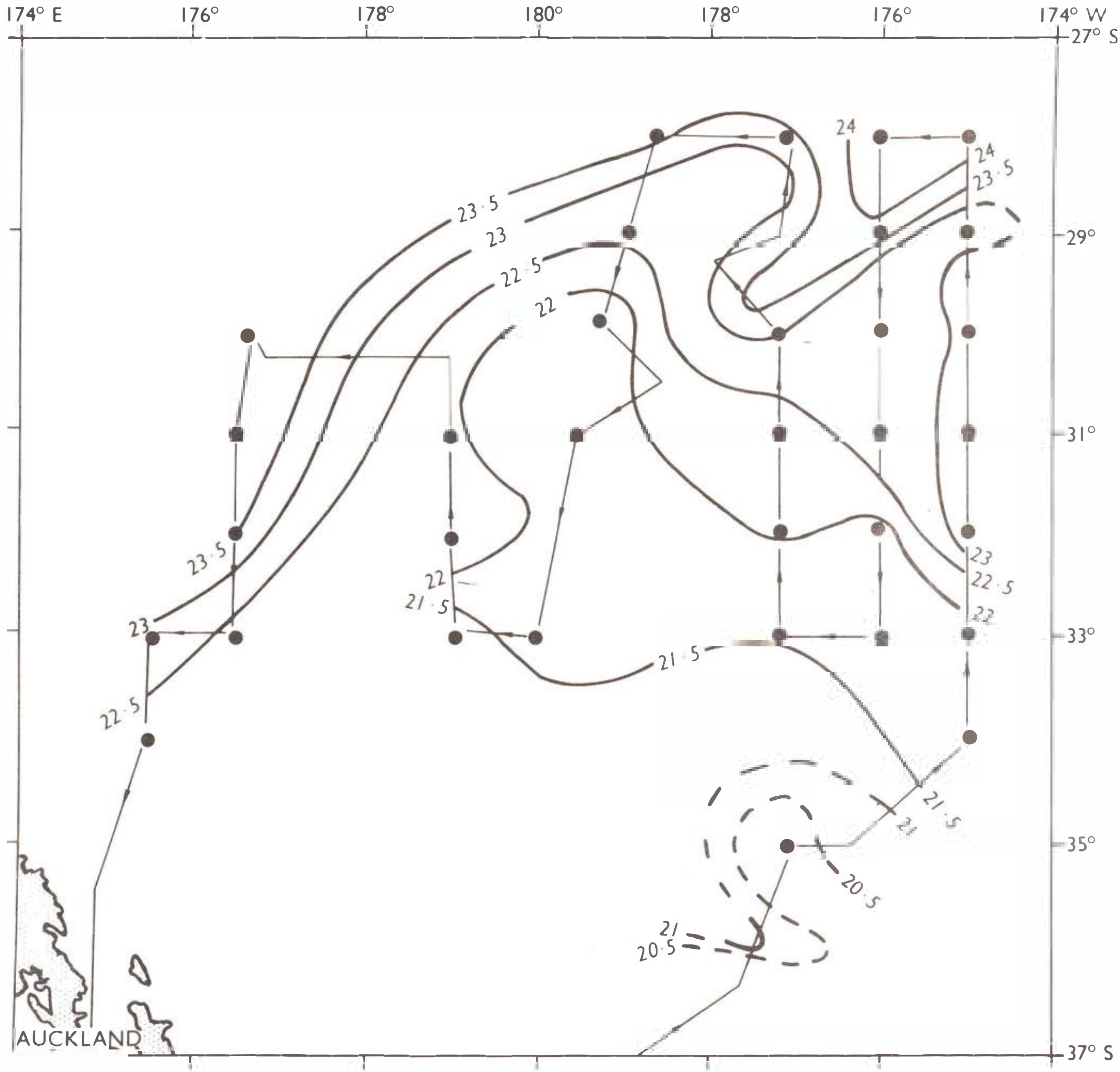

Fig. 4. Distribution of surface isotherms (°C). The thin line with arrows represents the track of MV *Taranui.*

values of about 24°C and 35.35‰. These maximum values were not coincident however, the maximum temperature being found at Stn D704 in the northeast of the survey area and the maximum salinity about 335 km to the south of Stn D701.

A large tongue of relatively cool water was directed towards the northwest and a smaller tongue of warmer water was directed towards the southwest (Fig. 4). The salinity distribution showed a somewhat different pattern (Fig. 5). A large tongue of water was directed towards the southwest (indicated by the 35.7‰ isohaline) with an intrusion of higher salinity water (35.85‰) from the east at about latitude 31°S and an intrusion of lower salinity water (35.65‰) from the east at about latitude 29°S. A strong salinity gradient was present between 32° and 34°S. The near-surface maximum salinity isohalines (Fig. 5) formed a pattern similar to that of the surface isohalines.

Upper Mixed Layers

Isobaths of the depth of the upper mixed layer (i.e. depth to the top of the seasonal thermocline) are shown in Fig. 6, the depths being taken from the bathythermograph traces (Fig. 7). This layer had an average thickness of about 43 m, varying between 30 m and 65 m. The maximum thickness was associated with a patch of high salinity near-surface water (Fig. 5) which suggests that the water in the upper mixed layer, at this position, had been transported from the northeast where a source of high salinity water (> 36.00‰) exists between approximately 10° and 30°S and 100° and 170°W (Muromtsev 1963, fig. 134).

Temperature and Salinity at 200 m Depth

The well-developed tongue of surface water which extended southwestwards (Figs 4, 5) was not so evident at 200 m (Figs 8, 9) which suggests that water in this near-surface tongue had been transported from the northeast by the Trade Wind Drift to about latitude 33°S. Monthly charts of average surface currents for the summer months of January to March compiled from ships' observations (Wyrtki 1960)

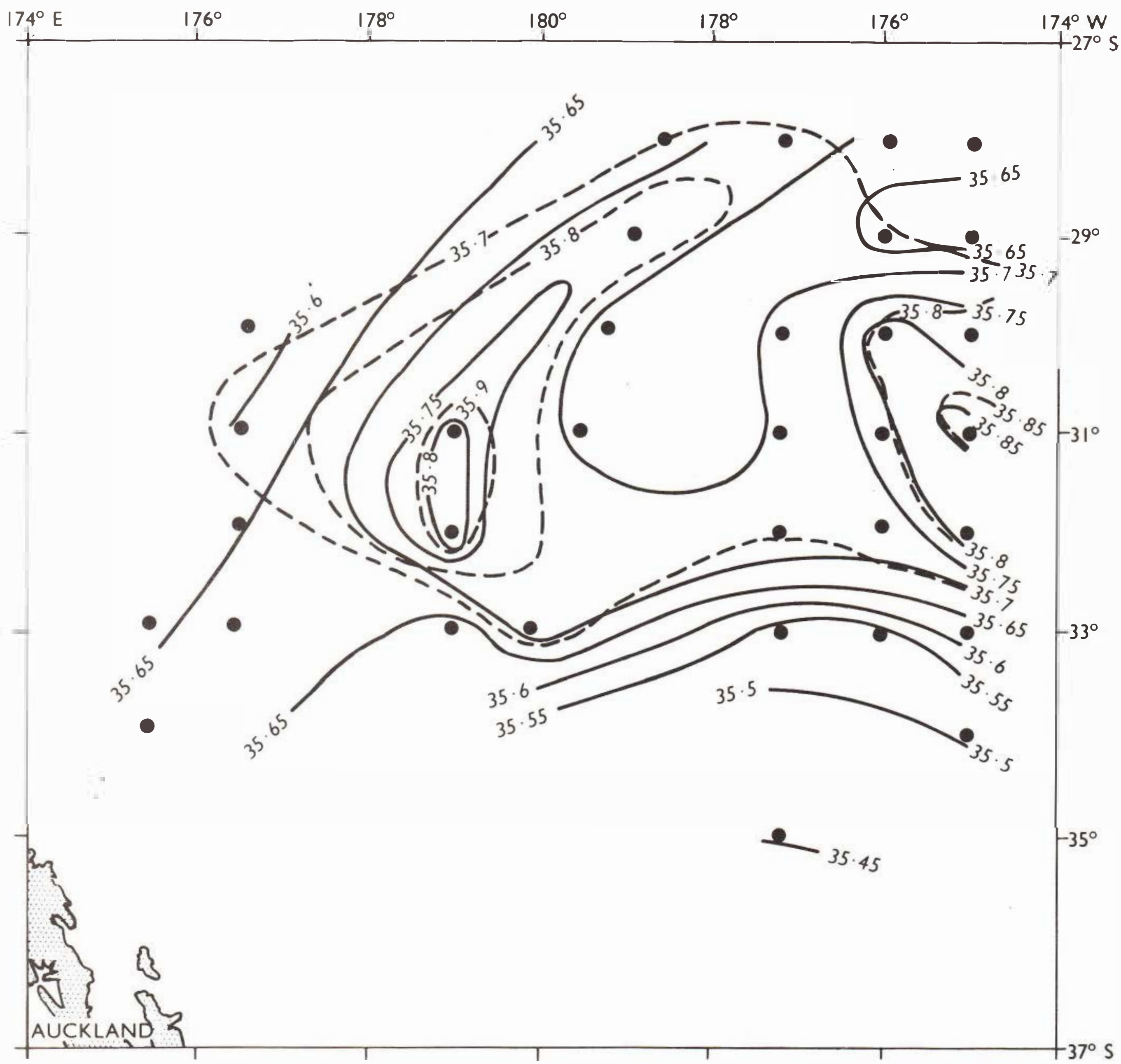

Fig. 5. Distribution of surface isohalines (‰), full lines. Where broken lines diverge from full lines they represent isohalines of the near-surface salinity maximum.

show a southwesterly flow between latitudes 10°S and 30°S. This direction is almost opposite to that of the geostrophic flow (*see* Fig. 2, also Garner 1969) and Wyrtki (1962) stated that, since the Trade Wind Drift is confined to the surface waters, it cannot appear as a geostrophic current. Commenting upon this, Garner (1970, p. 10-11) remarks that "this implies a special, almost completely ageostrophic situation". Results of the present survey show an example of this phenomenon. The effect of wind stress on geostrophic flow is considered below.

Following Reid (1961), by eliminating the Coriolis term between the momentum equations including the horizontal pressure, Coriolis, and vertical shearing stress terms we have

$$u\alpha \frac{\partial p}{\partial x} + v\alpha \frac{\partial p}{\partial y} = u\alpha \frac{\partial \tau_x}{\partial z} + v\alpha \frac{\partial \tau_y}{\partial z} \qquad (1)$$

where τ_x, τ_y, are the horizontal stress components, p the pressure, α the specific volume and (u, v) the velocity components positive in the x

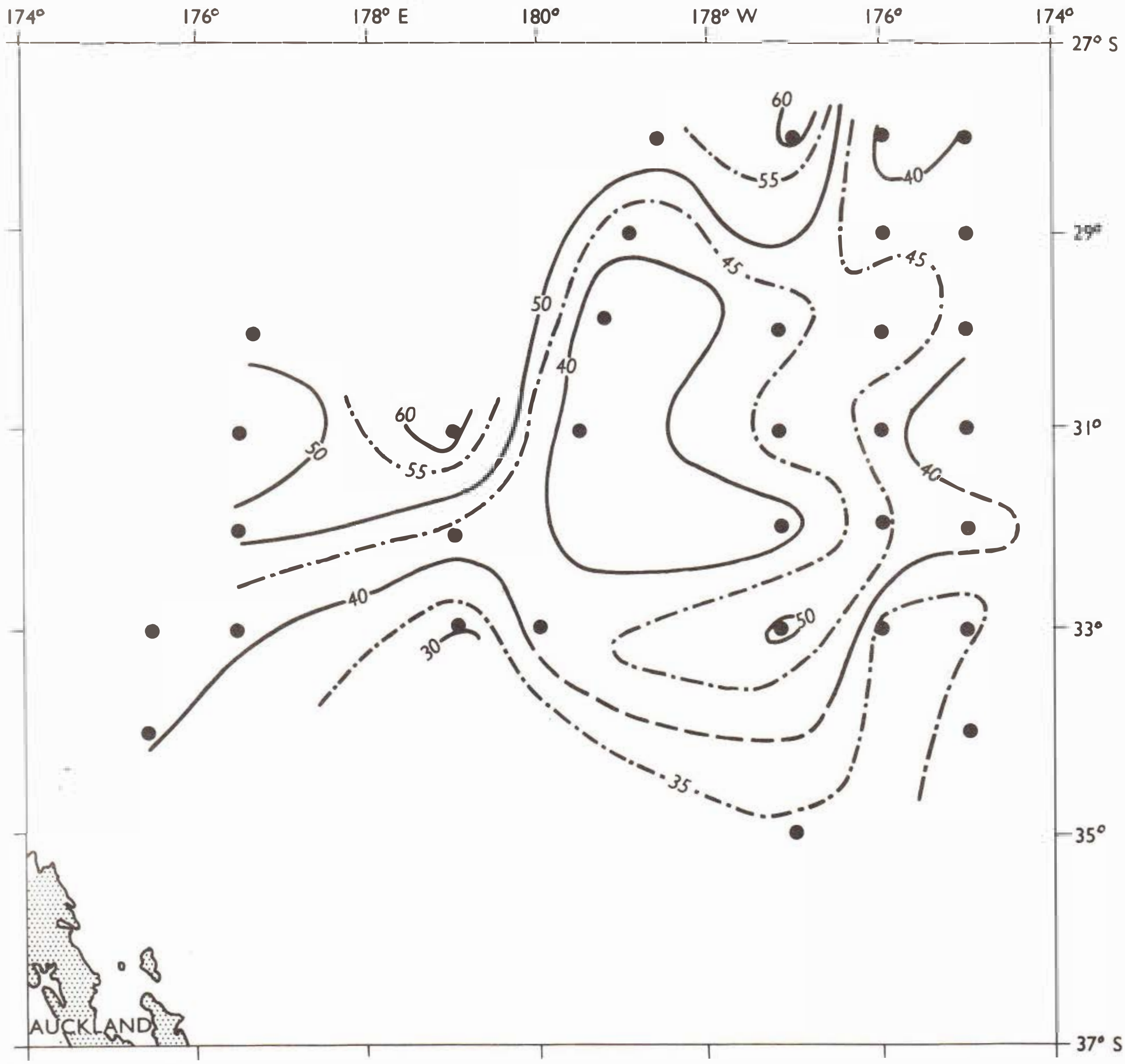

Fig. 6. Isobaths (metres) of the depth of the upper mixed layer.

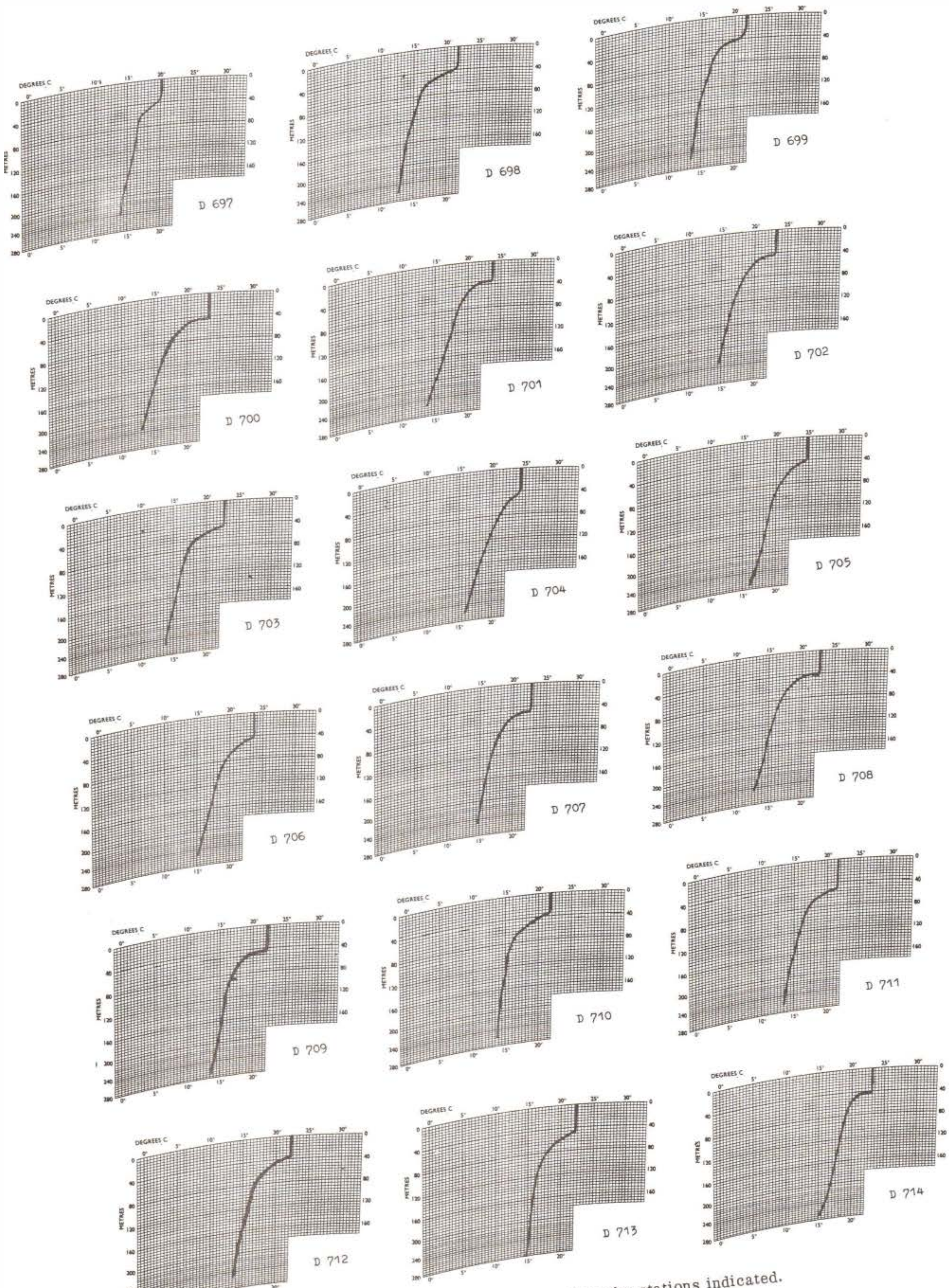

Fig. 7. Bathythermograph traces from the stations indicated.

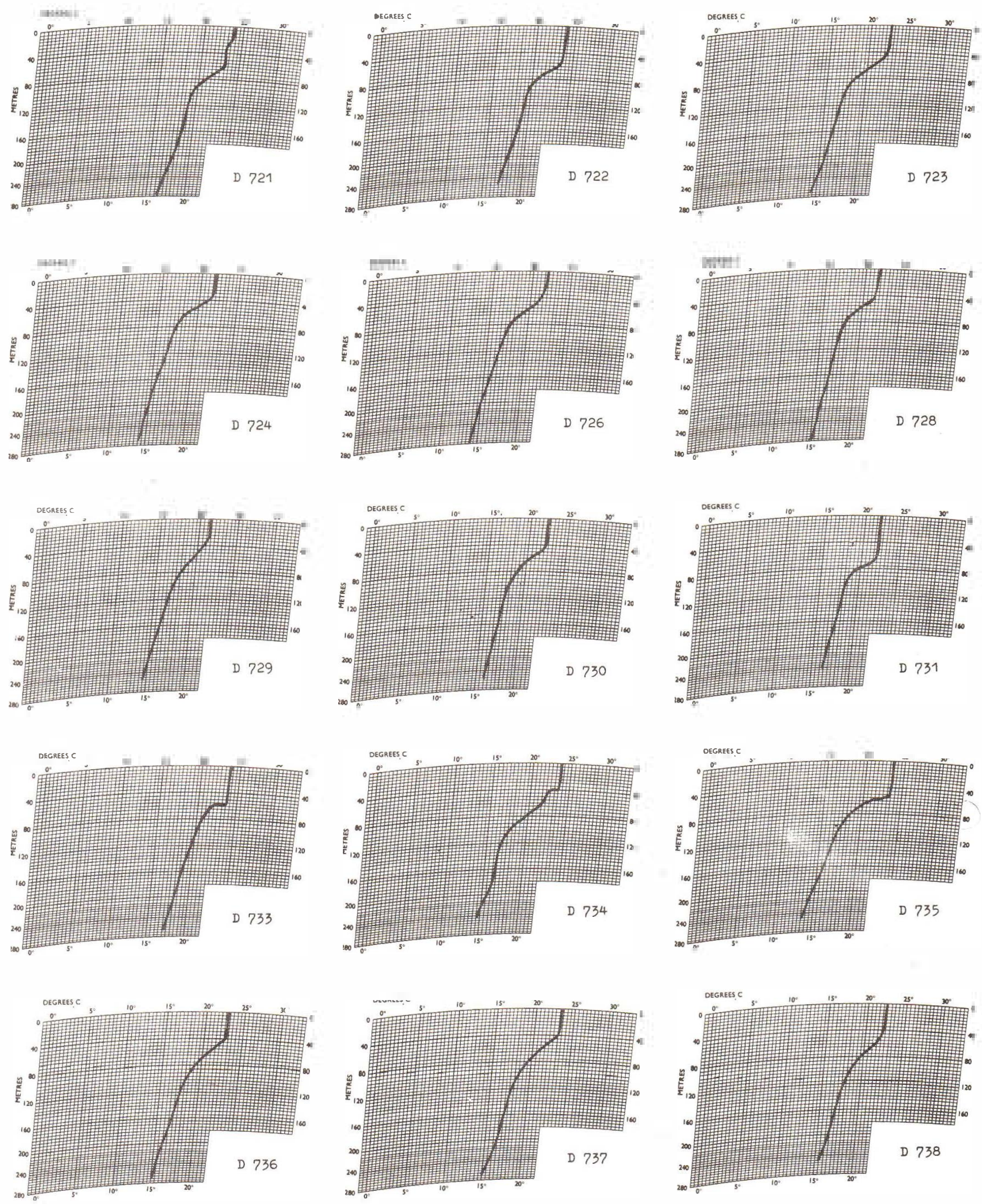

Fig. 7 - *continued.*

(east) and y (north) directions respectively. Assuming that the time rate of change of the geopotential difference is zero, this equation expresses the change in geopotential along a streamline as related to the vertical shearing stress. Say for convenience we assume that the flow is zonal (alternatively one axis could be orientated along the direction of flow) equation 1 reduces to

$$\alpha \frac{\partial p}{\partial x} - \frac{\partial D}{\partial x} = \alpha \frac{\partial \tau_x}{\partial z} \qquad (2)$$

where D, the dynamic height anomaly, is given by

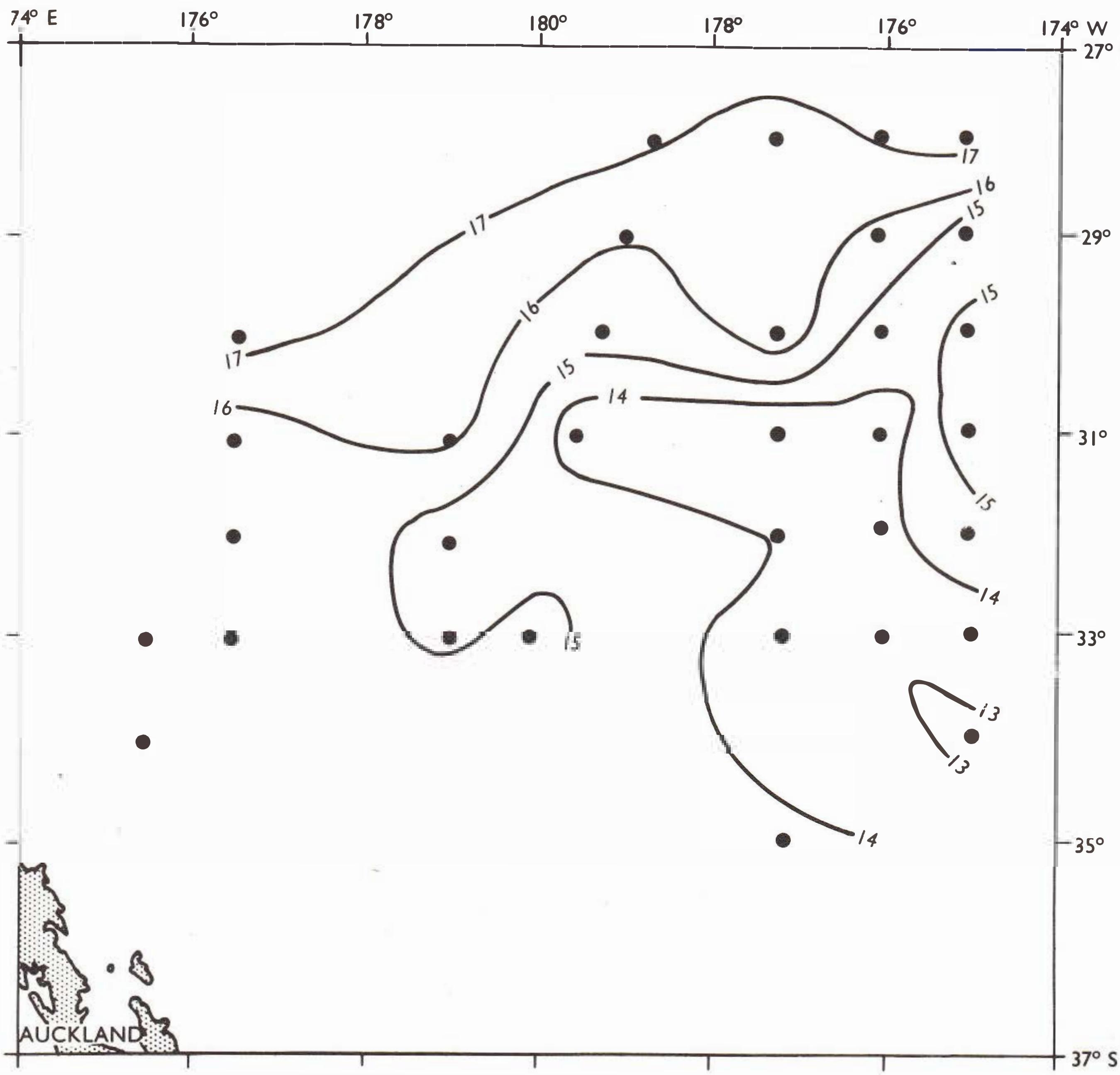

Fig. 8. Distribution of isotherms (°C) at a depth of 200 m.

$$D = \int_{p}^{p_H} \alpha \, dp,$$

where p_H is the pressure at the reference surface which is taken here as 1000 dbars. Assuming that the direct influence of the wind is confined to the upper 100 m of the ocean and approximating

$$\int_{0}^{1000} \frac{1}{\alpha} \frac{\partial D}{\partial x} \, dz$$

by $\frac{1}{\alpha} \frac{\Delta D}{\Delta x_S} 50$ where ΔD is the change in the dynamic height anomaly at the surface over a longitudinal distance Δx_S, $\bar{\alpha}$ the average specific volume in the upper 100 m, then on integrating equation 2 with respect to depth over the upper 100 m gives

$$\frac{1}{\bar{\alpha}} \frac{\Delta D}{\Delta x_S} \times 50 = (\tau_x)_0 \qquad (3)$$

where $(\tau_x)_0$ is the surface wind stress. The relevant wind stress data in 5° squares for the months December-February taken from Hidaka (1958) are given in

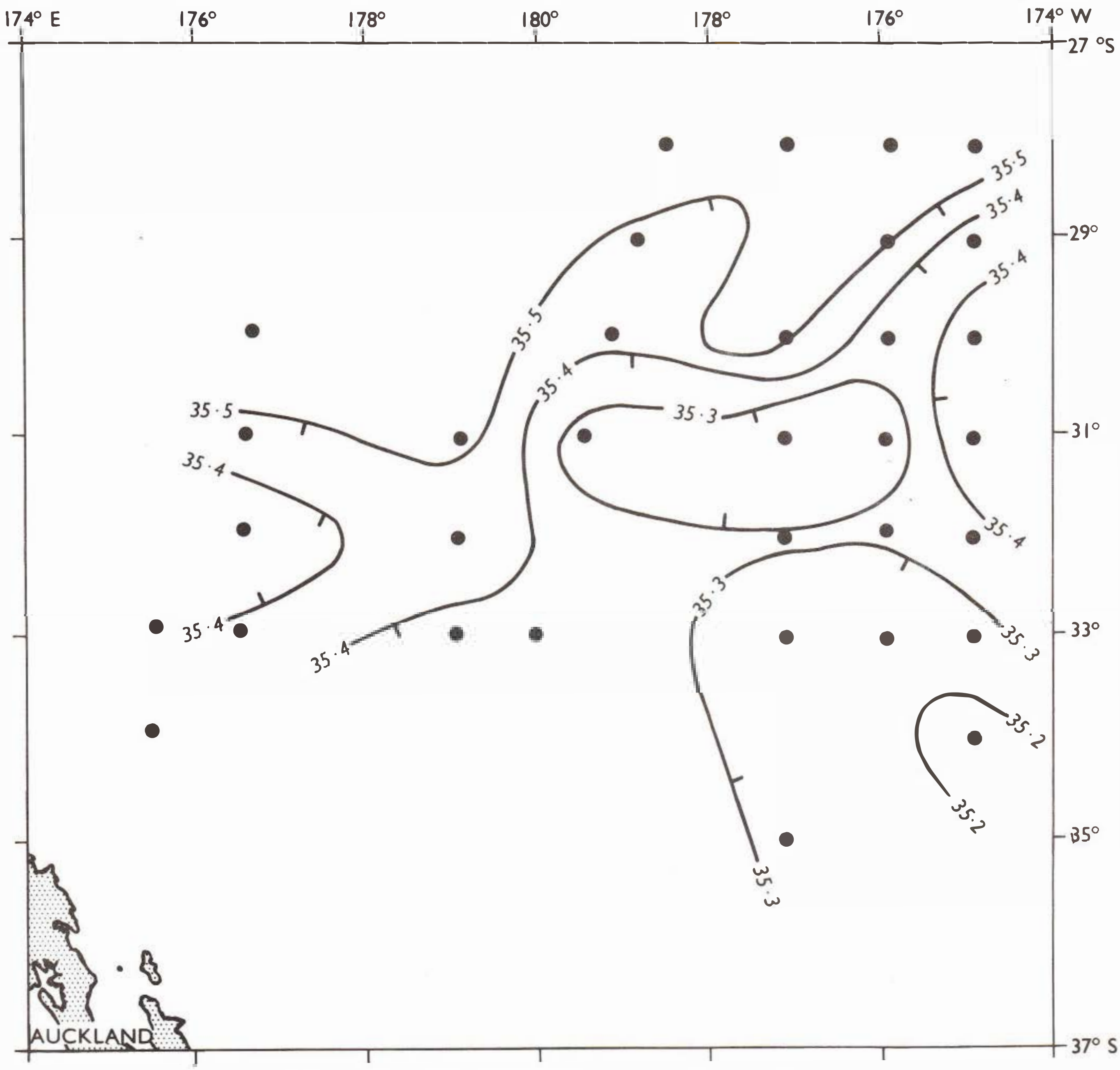

Fig. 9. Distribution of isohalines (‰) at a depth of 200 m.

Table 2. For a zonal wind stress of $-0.05\ \mathrm{N\,m^{-2}}$ (Table 2) with a value of $10^{-3}\ \mathrm{m^3\,kg^{-1}}$ for $\bar{\alpha}$, the longitudinal distance Δx_S to be covered to give a change in the dynamic height anomaly of -0.1 dyn m (= 1 M.K.S. unit) calculated from equation 3 is

TABLE 2

Wind stresses (τ) in 5° square northeast of New Zealand averaged over the period December-February as given by Hidaka (1958). Co-ordinates shown are those of the centres of the 5° squares. Stress components ($\mathrm{N\,m^{-2}} \times 10^{13}$) $(\tau_x)_0$ $(\tau_y)_0$ are positive to the east and north respectively.

		177.5°E	177.5°W
27.5°S	$(\tau_x)_0$	-50	-61
	$(\tau_y)_0$	+12	+ 7
32.5°S	$(\tau_x)_0$	-37	-27
	$(\tau_y)_0$	- 8	-10
37.5°S	$(\tau_x)_0$	16	41
	$(\tau_y)_0$	- 2	-15

1000 km. To give some estimate of the angle that the flow would then make with the dynamic height contours we take the data near 179°E where there is a change of 0.1 dyn m in a distance of 170 km (1.5 - 1.7 dyn m contours along 179°E, Fig. 2, giving a geostrophic current of 6 cm sec^{-1} towards the north-east). However from the estimates above the actual current will make an angle of $\sin^{-1} 170/1000 = 10°$ to the right of the dynamic height anomaly contours. For a more general value for the Southwest Pacific Ocean, we may take a spacing of 2.5° latitude for a 0.1 dyn m change (Reid 1961, fig. 1) which gives an angle of 15° south of east. This estimate shows that the effect of the current flowing down the geopotential contours would account for at least part of the discrepancy between the direction of the geostrophic currents and the observed drift in this particular region.

Furthermore, the ageostrophic entry of Trade Wind Drift water would cause a northwards displacement of the calculated position of the boundary between the westward and eastward directed geostrophic currents because the water of the Trade

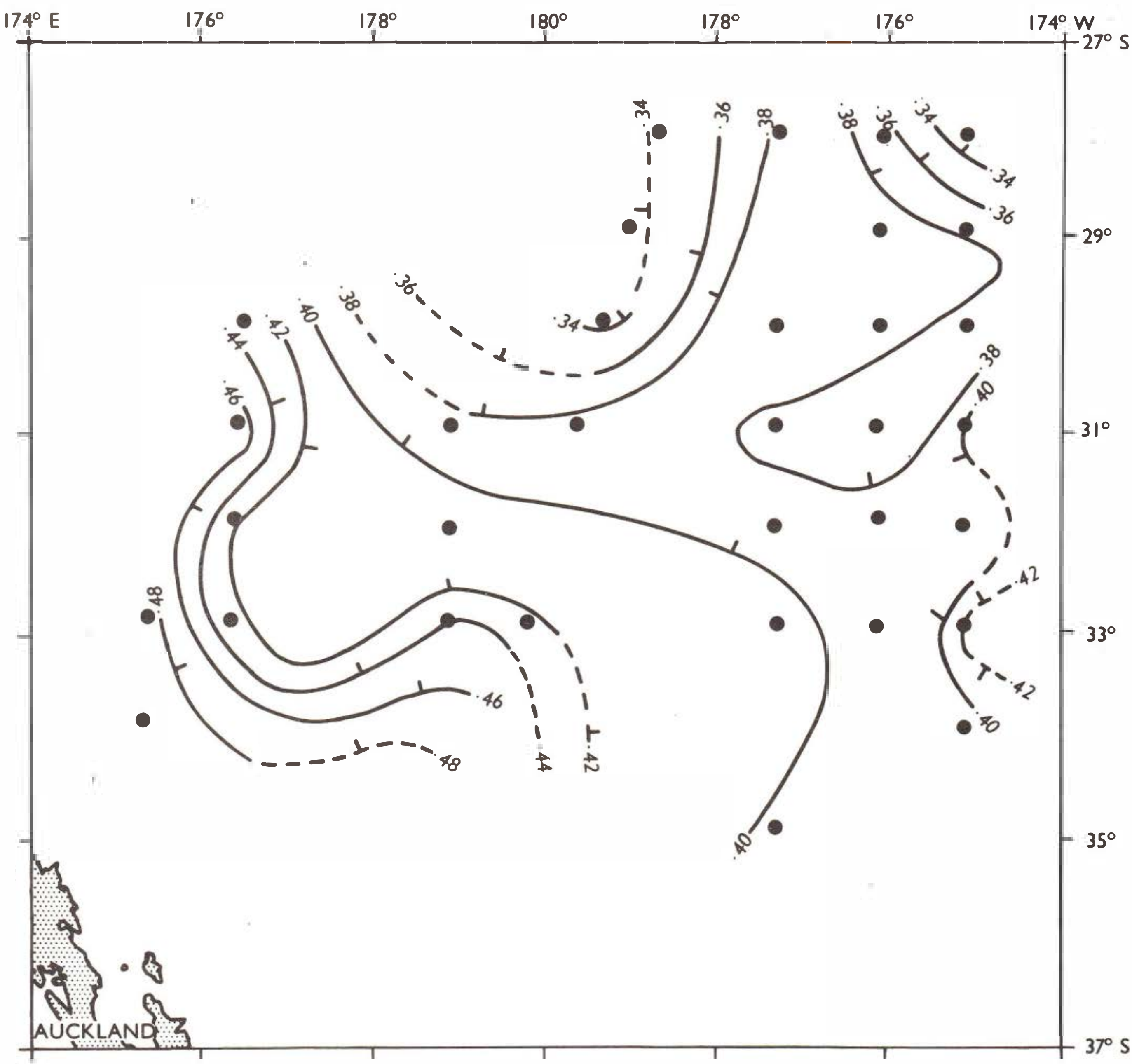

Fig. 10. Distribution of isohalines (‰) of minimum salinity. Contour values should be increased by 34‰.

Wind Drift immediately north of the region is generally lighter and has a thicker upper mixed layer than has the water further south.

A tongue of relatively cool water directed towards the northwest was present at 200 m (Fig. 8), a feature similar to that found at the surface (Fig. 4). A tongue of low salinity water (⩽ 35.3‰) at 200 m also extended northwestwards from the southeast of the survey area (Fig. 9). These tongues most likely originated from water which had turned northeast at East Cape on the east coast of New Zealand (*see* Garner 1969, fig. 4) and reflect the adjustment of the mass field to the currents. The water which turns northeast at East Cape itself originates from water of the East Australian Current system which has flowed eastwards across the Tasman Sea and rounded the north of New Zealand before moving southeastwards down the east coast to East Cape. This water can therefore be described as subtropical but, because of modifications during its long passage, its properties are different from the subtropical water transported by the Trade Wind Drift towards the northeast of New Zealand.

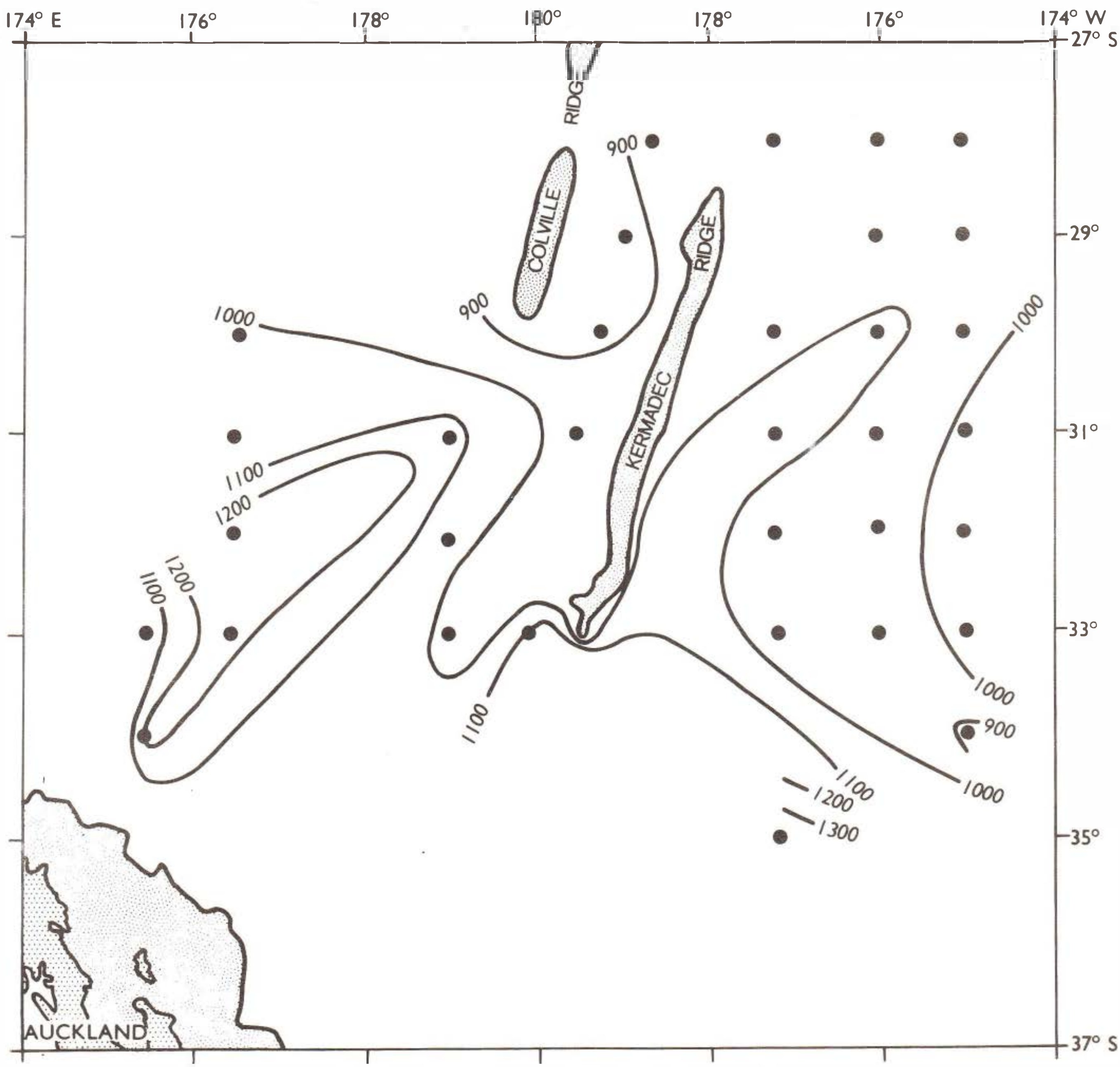

Fig. 11. Isobaths (metres) of the depth of the minimum salinity.

By definition, between these two components of circulation - the water derived from the East Australian Current system and the Trade Wind Drift - the Tropical Convergence is located. Stanton (1969) states that this convergence reaches its most southerly limit of latitude 30°S in January-March. During the present survey the Tropical Convergence was not at all well developed, although by definition it would be taken as approximately at the 35.7‰ surface isohaline (Fig. 5). Generally, the Tropical Convergence would be better defined north of North Cape, New Zealand, where the east-going flow from the Tasman Sea is confined to a narrower latitudinal extent, than it is to the northeast of New Zealand.

Antarctic Intermediate Water

Isohalines of the minimum salinity layer are shown in Fig. 10 and isobaths of the deptn of this layer in Fig. 11. This salinity minimum marks the core of Antarctic Intermediate Water. The depth of the layer varied from about 900 m in the southeast and northwest to about 1200 m in the southwest of the survey area (Fig. 11). The core layer salinity increased from 34.34‰ in the northeast, with some intrusion of water (⩾34.40‰) from the east at about latitude 33°S (Fig. 10). The data here have been used in an analysis of the distribution of minimum salinity water around New Zealand (Heath 1972).

Vertical Profiles of Temperature and Salinity

The vertical distributions of temperature and salinity are illustrated for two cross sections (Figs 12, 13). The meridional temperature and salinity sections along 177°W (Fig. 12) show a marked slope in the isolines between Stns D713 and D714 at depths between about 100 m and 700 m. This indicates that the water at any level between these depths was warmer and more saline at the two northern stations (D721, D714) than at the stations further south. Similarly, in the zonal sections (Fig. 13) the water at the two western stations (D734, D731), at any depth between about 100 m and 1000 m (i.e., the approximate depth of the core of Antarctic Intermediate Water), was warmer and more saline than at the stations to the east, with the exception of the most easterly station, D701.

The salinity increased with depth below the Antarctic Intermediate Water, but the sampling did not extend to depths sufficient to define the salinity maximum marking the core of Deep Water. The station spacing over the Kermadec Trench was too great to detect any northward flow of Deep Water such as reported by Reid *et al* (1968).

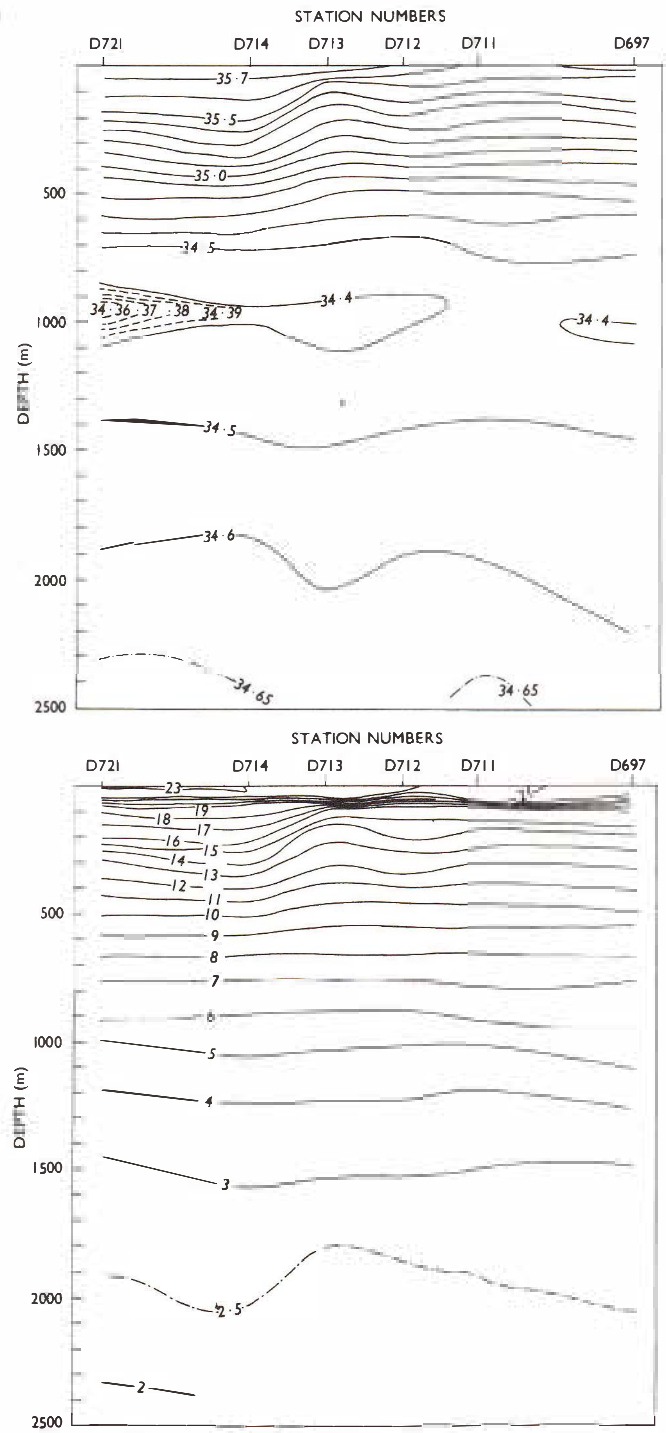

Fig. 12. Vertical meridional cross section of temperature (bottom, °C) and salinity (top, ‰).

Sound Velocity

As in previous surveys in the present series (Garner 1967a, b; 1970; Ridgway 1970) values of sound velocity have been computed and the corrections to be applied to an echo sounding machine calibrated for a velocity of 1500 ms^{-1} have been derived

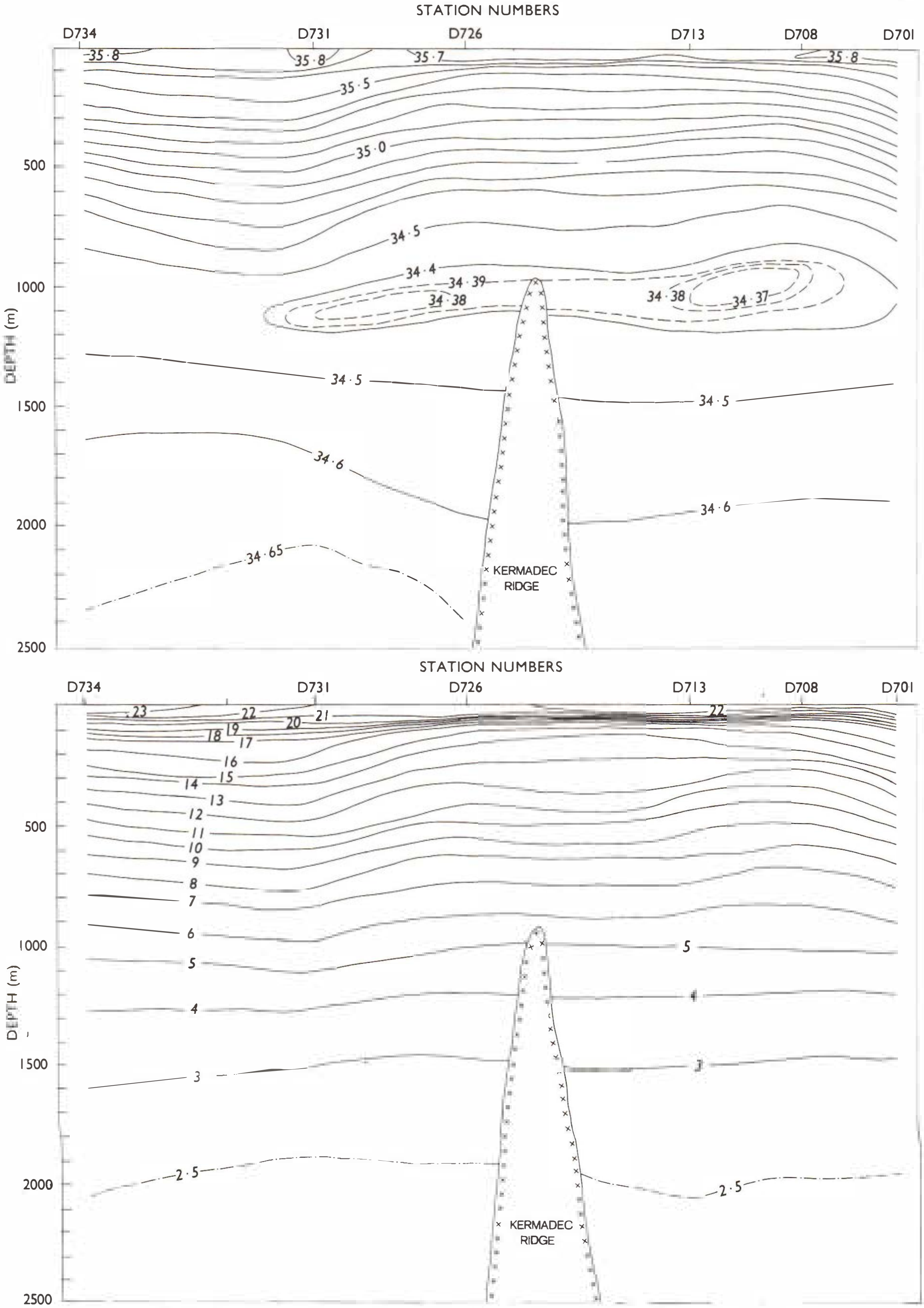

Fig. 13. Vertical zonal cross section of temperature (bottom, °C) and salinity (top,‰).

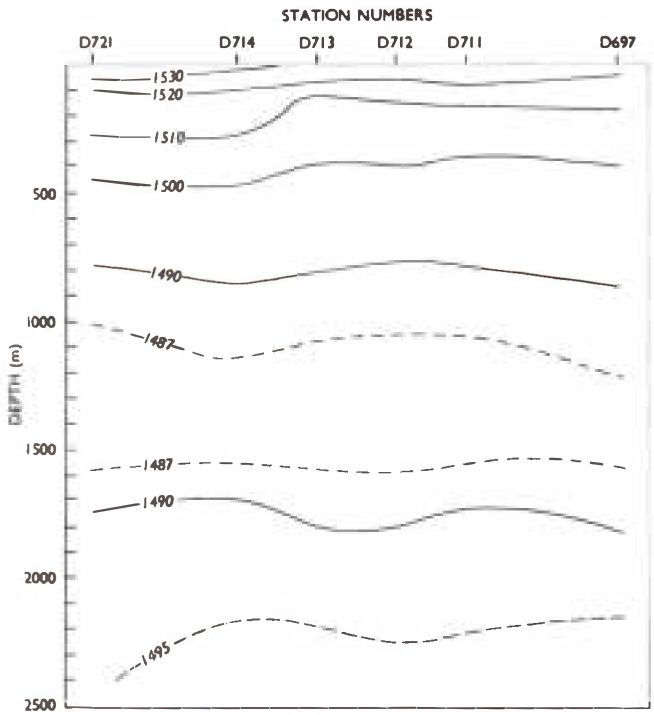

Fig. 14. Vertical meridional cross section of sound velocity (metres per second).

(*see* Appendix). A meridional cross section showing the vertical distribution of sound velocity is illustrated in Fig. 14. The sound velocity decreased with depth until minimum velocities marking the SOFAR channel were reached at depths of 1200-1300 m. The sound velocities in this channel varied from 1485 (Stns D711 and D721) to 1487 m s^{-1}. The slope of the isotherms and isohalines between Stns D713 and D714 previously noted are reflected in the isopleths of sound velocity.

Garner (1967c) has described the configuration of the sound channel around New Zealand and the sound velocities determined here further supplement his work.

The echo sounder corrections derived from the observed data are generally somewhat smaller (by about 5 m s^{-1} at a depth of 2000 m) than those shown for the region by Matthews (1939).

CONCLUSION

The results of this first hydrological study of the Kermadec Region show that the surface geostrophic flow relative to 1000 dbars is consistent with the broader geostrophic circulation patterns shown by Reid (1961) and Wyrtki (1962) which cover this area and is continuous with the geostrophic circulation shown by Garner (1969). The northern part of the survey region lies within the Trade Wind Drift as shown on current atlases and an explanation for the discrepancies between the directions of the observed drift and the geostrophic flow is advanced. The direct effect of the wind on the geostrophic flow results in the water flowing downhill and the indirect effect of the wind on the geostrophic flow is to bring Trade Wind Drift water south, with the result that in the geostrophic computations the boundary between the oppositely directed geostrophic currents is placed further north than its equilibrium position.

ACKNOWLEDGMENTS

The field assistance given by Messrs B.J. Fowke, N.H. Lambert and N.D. Robertson, of the N.Z. Oceanographic Institute, is gratefully acknowledged. Thanks are also due to the officers and crew of MV *Taranui* (Capt. R.D. Matheson). Computing facilities were provided by the Applied Mathematics Division, of D.S.I.R. Wellington and figures were prepared for publication by the Cartographic Section, D.S.I.R., Wellington.

REFERENCES

BROWN, H.L.; HAMON, B.V. 1961: An inductive salinometer. *Deep Sea Res. 8(1)* : 65-75.

CULBERTSON, M.F. 1955: An oceanographic slide rule for computing temperature, depth and salinity. *Trans. Am. geophys. Un. 36(3)* : 473-80.

GARNER, D.M. 1967a: Hydrology of the Southern Hikurangi Trench Region. *Mem. N.Z. oceanogr. Inst. 39. (Bull. N.Z. Dep. scient. ind. Res. 181).*

GARNER, D.M. 1967b: Hydrology of the South-east Tasman Sea. *Mem. N.Z. oceanogr. Inst. 48. (Bull. N.Z. Dep. scient. ind. Res. 181).*

GARNER, D.M. 1967c: Oceanic sound channels around New Zealand. *N.Z. Jl mar. Freshwat. Res. 1(1)* : 3-15.

GARNER, D.M. 1969: The geopotential topography of the ocean surface around New Zealand. *N.Z. Jl mar. Freshwat. Res. 3(2)* : 209-19.

GARNER, D.M. 1970: Hydrological studies in the New Zealand region 1966 and 1967. *Mem. N.Z. oceanogr. Inst. 58. (Bull. N.Z. Dep. scient. ind. Res. 202).*

HEATH, R.A. 1972: Choice of reference surface for geostrophic currents around New Zealand. *N.Z. Jl mar. Freshwat. Res. 6(1 & 2)* : 148-77.

HIDAKA, K. 1958: Computation of the wind stresses over the oceans. *Rec. oceanogr. Wks Japan 4(2)* : 77-123.

LAFOND, E.C. 1951: Processing oceanographic data. *Publs U.S. hydrogr. Off. 614.* 114 pp.

MATTHEWS, D.J. 1939: Tables of the velocity of sound in pure water and sea water for use in echo sounding and sound ranging. *Publs Admiralty hydrogr. Dep. 282.* 151 pp.

MUROMTSEV, A.M. 1963: "The Principal Hydrological Features of the Pacific Oceans". Israel Program for Scientific Translations, Jerusalem. 417 pp. *(Translation of* Osnovnye chertygidrolgi Tikhogo okeana, Gidrometeorologischeskoe I-date'stvo, Leningrad, 1958).

NATIONAL INSTITUTE OF OCEANOGRAPHY OF GREAT BRITAIN AND UNESCO, 1966: "International Oceanographic Tables". UNESCO, Paris, France. 128 pp.

NEUMANN, G. 1960: On the effect of bottom topography on ocean currents. *Dt. hydrogr. Z. 13(3)* : 132-41.

REID, J.L. 1961: On the geostrophic flow at the surface of the Pacific Ocean with respect to the 1000 decibar surface. *Tellus 13(4)* : 489-502.

REID, J.L.; STOMMEL, H.; STROUP, E.; WARREN, B. 1968: Detection of a deep boundary current in the western South Pacific. *Nature, Lond. 217* : 937.

RIDGWAY, N.M. 1970: Hydrology of the Southern Kermadec Trench Region. *Mem. N.Z. oceanogr. Inst. 56. (Bull. N.Z. Dep. scient. ind. Res. 205).*

STANTON, B.R. 1969: Hydrological observations across the Tropical Convergence north of New Zealand. *N.Z. Jl mar. Freshwat. Res. 3(1)* : 124-46.

WILSON, W.B. 1960: Speed of sound in sea water as a function of temperature, pressure and salinity. *J. acoust. Soc. Am. 32* : 641-4.

WYRTKI, K. 1960: The surface circulation in the Coral and Tasman Seas. *Tech. Pap. Div. Fish Oceanogr. C.S.I.R.O. Aust.* No. 8.

WYRTKI, K. 1962: Geopotential topographies and associated circulation in the western South Pacific Ocean. *Aust. Jl mar. Freshwat. Res. 13(2)* : 89-105.

APPENDIX

NUMERICAL STATION DATA

D is the thermometrically measured pressure in decibars at each sampling point. This is numerically nearly equal to the geometric depths in metres. A more accurate conversion using representative mean density figures (LaFond 1951, p.8) is as follows:-

pressure (decibars)	200	400	600	800	1000	1500	2000	2500
depth (metres) :	199	398	595	793	991	1484	1976	2467

T is the sample temperature in °C x 100.

S is the sample salinity in ‰ x 100.

σ_t is the water density reduced to surface pressure isothermally x 100.

σ_{stp} is the *in situ* water density.
The "σ" value is derived from the density, ρ, from the relationship $\sigma = (\rho-1) \times 10^5$ where ρ is the water density in g cm^{-3}.

$\Sigma\Delta D$ is the cumulative anomaly of the geopotential distance between the sea surface and the sample depth in dynamic centimetres.

C is the *in situ* sound velocity in m s^{-1} x 10.

Cm is the integral mean sound velocity between the sea surface and the sample depth in m s^{-1} x 10.

K is the correction, in metres x 10, to be applied to an echo sounding of a depth corresponding to the depth D on a machine calibrated for a velocity of 1,500 m s^{-1}.

$\Sigma\Delta X = \int_{\rho}^{0} \delta \, dp$ is the potential energy anomaly from the sea surface to the sample depth in kg m s^{-4} x 10^3 (p is the pressure and δ the specific volume anomaly giving the difference between the actual specific volume and that in a standard ocean at temperature 0°C and salinity at 35‰).

D	T	S	σ_t	σ_{stp}	$\Sigma\Delta D$	C	C_m	K
D697								
0	2018	3545	2508	2508	0.0	15231	15231	0
29	2017	3551	2512	2525	8.3	15237	15234	5
88	1645	3546	2601	2641	22.7	15139	15203	12
118	1585	3543	2613	2665	28.6	15125	15185	15
166	1494	3535	2627	2701	37.6	15103	15164	18
225	1380	3523	2642	2743	47.9	15075	15144	22
379	1112	3492	2671	2841	71.8	15005	15102	26
616	845	3458	2690	2968	104.2	14942	15052	21
823	668	3445	2705	3079	129.7	14905	15020	11
1056	515	3439	2720	3201	155.4	14882	14992	-6
1345	348	3447	2744	3359	182.2	14860	14965	-31
1575	296	3453	2754	3474	200.0	14878	14951	-51
1817	266	3456	2759	3587	217.6	14905	14943	-69
1944	258	3458	2761	3646	226.6	14923	14941	-76
2456	218	3462	2767	3879	262.5	14993	14945	-90
D698								
0	2158	3550	2473	2473	0.0	15269	15269	0
25	2169	3550	2470	2481	8.0	15277	15273	5
49	1820	3543	2557	2579	14.9	15184	15252	8
74	1571	3540	2614	2647	20.3	15114	15217	11
98	1464	3537	2635	2679	24.7	15083	15188	12
153	1385	3528	2645	2714	33.8	15066	15147	15
269	1177	3500	2665	2786	51.8	15010	15100	18
332	1076	3487	2674	2823	60.8	14984	15080	18
489	878	3461	2687	2908	81.9	14934	15041	13
727	689	3442	2700	3030	111.6	14897	14999	-0
880	548	3438	2715	3116	129.0	14866	14979	-12
1210	400	3442	2735	3288	161.3	14860	14947	-43
1429	319	3450	2749	3403	179.5	14863	14934	-63
1666	281	3454	2756	3517	197.1	14886	14925	-83
1910	253	3457	2761	3631	214.5	14915	14922	-99
2372	216	3467	2772	3847	245.6	14978	14927	-115
D699								
0	2166	3561	2480	2480	0.0	15273	15273	0
28	2152	3561	2483	2496	8.8	15274	15273	5

D	T	S	σ_t	σ_{stp}	$\Sigma\Delta D$	C	C_m	K
D699 continued								
55	1868	3553	2553	2577	16.4	15200	15255	9
80	1648	3549	2603	2639	22.0	15138	15228	12
106	1530	3544	2626	2673	26.9	15106	15202	14
151	1440	3536	2640	2707	34.8	15083	15170	17
206	1334	3526	2654	2746	43.7	15057	15143	20
280	1227	3515	2667	2793	54.8	15032	15117	22
487	956	3478	2687	2907	83.2	14965	15066	22
754	704	3451	2705	3047	116.0	14909	15020	10
959	551	3443	2718	3155	138.6	14881	14993	-4
1234	384	3446	2740	3304	181.8	14861	14949	-49
1610	273	3459	2760	3497	192.7	14874	14941	-63
1950	249	3462	2765	3653	215.3	14921	14933	-86
2436	218	3465	2770	3873	247.8	14990	14938	-101
D700								
0	2324	3582	2451	2451	0.0	15315	15315	0
27	2322	3585	2453	2465	9.2	15320	15317	6
54	2320	3582	2452	2475	18.5	15324	15319	12
81	1799	3561	2576	2612	26.2	15185	15298	16
101	1683	3555	2599	2644	30.5	15153	15272	18
137	1585	3548	2617	2678	37.6	15129	15237	22
181	1498	3540	2630	2711	45.7	15108	15208	25
250	1369	3525	2646	2758	57.6	15076	15176	29
310	1257	3512	2659	2798	67.1	15047	15154	32
436	1071	3487	2675	2870	85.7	15000	15116	34
679	756	3450	2697	3004	117.8	14916	15059	27
864	620	3440	2707	3100	139.8	14892	15025	15
1102	469	3439	2725	3228	165.2	14869	14994	-4
1298	358	3445	2741	3335	183.1	14856	14974	-23
1485	305	3452	2752	3432	197.8	14867	14960	-40
1646	270	3457	2759	3512	209.3	14879	14951	-54
1991	235	3460	2764	3672	232.6	14921	14942	-77
D701								
0	2322	3586	2454	2454	0.0	15315	15315	0
23	2319	3587	2456	2466	7.8	15318	15316	5
46	2255	3584	2472	2492	15.4	15306	15314	10

D701 continued

D	T	S	σ_t	σ_{stp}	$\Sigma\Delta D$	C	C_m	K
70	2068	3564	2509	2539	22.8	15258	15303	14
92	1817	3562	2572	2613	28.5	15192	15284	17
101	1782	3561	2580	2625	30.6	15183	15276	19
156	1659	3556	2606	2675	42.3	15155	15238	25
234	1532	3544	2626	2730	57.3	15128	15206	32
269	1465	3536	2634	2754	63.6	15110	15194	35
387	1239	3511	2662	2835	83.1	15053	15160	41
658	840	3460	2692	2989	121.2	14946	15093	41
870	632	3445	2710	3105	146.7	14899	15051	30
1018	514	3441	2721	3185	162.6	14875	15027	19
1191	416	3443	2734	3278	179.2	14864	15004	3
1382	332	3449	2747	3380	195.4	14860	14984	-14
1631	276	3455	2757	3503	213.9	14878	14967	-36
2098	237	3462	2766	3720	246.0	14940	14954	-65

D702

D	T	S	σ_t	σ_{stp}	$\Sigma\Delta D$	C	C_m	K
0	2314	3578	2450	2450	0.0	15312	15312	0
25	2319	3581	2451	2462	8.5	15318	15315	5
55	2037	3568	2520	2544	17.9	15249	15298	11
85	1842	3563	2567	2604	25.6	15199	15272	15
114	1706	3556	2595	2645	32.1	15163	15249	19
173	1597	3549	2615	2692	44.0	15139	15215	25
233	1486	3539	2632	2736	55.1	15113	15192	30
297	1360	3523	2647	2779	66.1	15079	15171	34
373	1226	3505	2660	2826	78.3	15045	15149	37
547	908	3466	2686	2933	103.3	14955	15101	37
837	623	3439	2706	3087	139.1	14888	15038	21
1044	468	3439	2725	3202	161.1	14861	15006	4
1343	335	3446	2744	3359	187.8	14854	14972	-25
1620	280	3453	2755	3496	208.9	14877	14954	-50
1881	261	3458	2761	3618	227.5	14914	14946	-68
2165	233	3463	2767	3751	246.9	14950	14944	-81
2622	202	3467	2773	3957	277.4	15015	14951	-86

D703

D	T	S	σ_t	σ_{stp}	$\Sigma\Delta D$	C	C_m	K
0	2257	3565	2457	2457	0.0	15296	15296	0
23	2254	3567	2459	2469	7.7	15299	15298	5
46	2253	3567	2460	2480	15.4	15304	15299	9
69	1825	3558	2567	2598	22.0	15190	15282	13
92	1649	3546	2601	2641	27.1	15140	15253	15
173	1447	3536	2638	2715	42.2	15090	15188	22
246	1347	3524	2650	2760	54.3	15067	15155	25
284	1275	3513	2656	2783	60.3	15048	15142	27
387	1083	3490	2675	2849	75.6	14996	15110	28
593	810	3454	2692	2960	103.0	14925	15058	23
945	535	3438	2716	3147	143.9	14870	14998	-2
1109	443	3441	2729	3236	160.3	14860	14978	-16
1282	359	3445	2741	3328	175.6	14855	14961	-33
2195	233	3464	2768	3765	243.9	14955	14938	-91

D704

D	T	S	σ_t	σ_{stp}	$\Sigma\Delta D$	C	C_m	K
0	2431	3567	2408	2408	0.0	15339	15339	0
29	2417	3563	2409	2421	11.1	15340	15340	7
58	2254	3569	2461	2486	21.6	15306	15331	13
87	2018	3565	2523	2561	30.5	15248	15313	18
115	1923	3565	2548	2598	37.9	15227	15295	23
161	1827	3565	2572	2643	49.2	15206	15272	29
214	1723	3557	2591	2686	61.1	15184	15253	36
315	1576	3543	2615	2754	82.0	15154	15226	47
364	1422	3524	2634	2796	91.2	15111	15213	52
514	1026	3475	2673	2904	115.5	14993	15166	57

D704 continued

D	T	S	σ_t	σ_{stp}	$\Sigma\Delta D$	C	C_m	K
800	637	3437	2703	3067	153.0	14889	15085	45
1021	492	3434	2718	3184	177.6	14865	15039	27
1312	348	3444	2742	3342	204.9	14855	14999	-1
1538	297	3452	2753	3456	222.6	14872	14979	-22
1768	274	3457	2759	3566	239.2	14900	14967	-39
2406	215	3463	2769	3859	283.5	14984	14960	-64

D705

D	T	S	σ_t	σ_{stp}	$\Sigma\Delta D$	C	C_m	K
0	2455	3566	2400	2400	0.0	15345	15345	0
29	2460	3567	2399	2412	11.4	15351	15348	7
58	2163	3569	2486	2512	21.6	15282	15332	13
87	1991	3568	2532	2570	30.0	15241	15309	18
116	1869	3563	2560	2611	37.4	15211	15288	22
161	1775	3560	2581	2652	48.0	15190	15264	28
219	1696	3555	2596	2693	60.6	15176	15242	35
324	1543	3541	2621	2764	81.8	15145	15216	47
361	1404	3524	2638	2799	88.6	15105	15206	50
805	644	3438	2703	3069	153.9	14891	15091	49
1021	510	3437	2719	3184	178.0	14873	15046	31
1321	366	3444	2740	3344	206.5	14864	15005	5
1549	307	3453	2753	3461	224.7	14878	14985	-15
1803	278	3456	2758	3580	243.4	14908	14972	-33
2052	256	3459	2762	3695	261.3	14940	14966	-46
2558	211	3464	2770	3926	296.8	15007	14968	-55

D706

D	T	S	σ_t	σ_{stp}	$\Sigma\Delta D$	C	C_m	K
0	2353	3563	2428	2428	0.0	15320	15320	0
25	2340	3566	2434	2445	9.0	15322	15321	5
53	2152	3570	2490	2513	18.4	15278	15310	11
82	1902	3567	2555	2591	26.4	15215	15287	16
111	1806	3564	2577	2625	33.3	15192	15265	20
163	1696	3558	2599	2671	44.7	15168	15238	26
292	1456	3539	2639	2768	69.3	15113	15195	38
349	1312	3520	2654	2810	78.8	15073	15178	41
512	985	3478	2683	2913	102.8	14979	15129	44
792	653	3443	2705	3065	137.9	14894	15060	32
1014	488	3450	2731	3195	160.9	14865	15020	14
1254	363	3445	2741	3315	181.9	14852	14989	-9
1510	288	3454	2755	3447	201.6	14863	14967	-34
1715	271	3457	2759	3543	216.0	14890	14956	-50
1930	246	3460	2764	3643	230.7	14916	14950	-64
2318	219	3464	2769	3821	256.6	14971	14949	-79

D707

D	T	S	σ_t	σ_{stp}	$\Sigma\Delta D$	C	C_m	K
0	2263	3580	2467	2467	0.0	15300	15300	0
23	2251	3581	2471	2481	7.5	15300	15300	5
50	2249	3580	2471	2492	16.3	15304	15301	10
77	1729	3558	2591	2625	23.5	15164	15277	14
103	1631	3554	2611	2657	28.8	15139	15245	17
154	1522	3543	2627	2696	38.4	15112	15205	21
217	1428	3533	2640	2737	49.4	15090	15175	25
250	1347	3522	2649	2760	54.9	15069	15162	27
316	1241	3509	2660	2801	65.3	15041	15140	29
456	987	3478	2682	2888	85.4	14971	15098	30
701	753	3453	2699	3017	116.7	14920	15045	21
1078	439	3440	2729	3222	157.1	14854	14989	-8
1286	333	3448	2746	3336	175.0	14844	14966	-29
1487	301	3452	2752	3433	190.2	14865	14951	-49
1705	284	3456	2757	3535	206.1	14894	14942	-66

D708

D	T	S	σ_t	σ_{stp}	ΣΔD	C	C_m	K
0	2267	3577	2463	2463	0.0	15300	15300	0
20	2267	3580	2465	2474	6.6	15304	15302	4
40	2271	3580	2464	2482	13.2	15308	15304	8
60	1877	3555	2552	2578	19.0	15203	15288	12
80	1691	3551	2594	2630	23.6	15152	15260	14
116	1564	3545	2619	2671	30.7	15119	15221	17
151	1477	3536	2632	2699	37.1	15095	15194	20
225	1315	3518	2652	2753	49.4	15053	15155	23
336	1117	3494	2672	2823	66.1	14999	15112	25
575	822	3458	2693	2953	98.0	14926	15050	19
738	665	3441	2702	3038	117.7	14889	15018	9
940	547	3437	2714	3143	140.5	14875	14989	-7
1125	443	3439	2728	3242	159.4	14863	14969	-23
1308	357	3445	2741	3340	175.8	14859	14954	-41
1502	298	3453	2753	3441	191.0	14866	14942	-58
1864	252	3460	2763	3613	216.3	14907	14931	-86

D709

D	T	S	σ_t	σ_{stp}	ΣΔD	C	C_m	K
0	2197	3573	2480	2480	0.0	15282	15282	0
26	2184	3567	2479	2490	8.2	15283	15282	5
52	1830	3554	2563	2586	15.4	15188	15259	9
78	1662	3550	2601	2635	21.2	15143	15228	12
104	1584	3546	2616	2662	26.3	15123	15204	14
146	1482	3538	2632	2697	33.9	15097	15177	17
199	1408	3532	2644	2732	43.0	15080	15153	20
264	1301	3520	2656	2774	53.4	15055	15132	23
331	1222	3509	2664	2812	63.6	15038	15144	25
466	984	3477	2682	2892	82.9	14972	15082	26
722	717	3447	2700	3027	115.5	14909	15032	15
947	583	3441	2713	3144	141.4	14892	15000	0
1163	415	3443	2734	3266	163.0	14858	14977	-18
1345	332	3450	2748	3364	178.2	14854	14960	-36
1515	304	3454	2754	3447	191.0	14872	14949	-51
1727	269	3458	2760	3549	206.0	14891	14941	-68
2110	229	3462	2767	3727	231.8	14939	14936	-90

D710

D	T	S	σ_t	σ_{stp}	ΣΔD	C	C_m	K
0	2171	3554	2473	2473	0.0	15273	15273	0
24	2126	3553	2485	2495	7.6	15264	15269	4
49	2087	3552	2494	2516	15.3	15259	15265	9
73	1650	3545	2600	2632	21.4	15137	15243	12
98	1494	3540	2631	2675	26.1	15093	15210	14
147	1407	3532	2644	2709	34.4	15072	15167	16
190	1328	3524	2654	2739	41.3	15051	15143	18
269	1201	3511	2669	2790	53.1	15019	15111	20
338	1113	3494	2672	2824	62.9	14999	15090	20
482	921	3471	2688	2905	82.3	14949	15056	18
727	713	3449	2702	3032	112.6	14907	15012	6
958	562	3440	2715	3151	138.8	14885	14984	-10
1206	401	3443	2735	3287	163.2	14859	14961	-31
1443	312	3451	2751	3411	182.6	14862	14944	-54
1675	277	3456	2758	3523	199.5	14886	14935	-73
1919	248	3460	2763	3638	216.3	14915	14930	-89
2392	212	3464	2770	3854	248.0	14979	14934	-106

D711

D	T	S	σ_t	σ_{stp}	ΣΔD	C	C_m	K
0	2149	3554	2479	2479	0.0	15267	15267	0
25	2130	3554	2484	2495	7.8	15267	15267	4
50	2128	3553	2484	2506	15.6	15270	15268	9
75	1694	3544	2588	2622	22.3	15152	15249	12

D711 continued

D	T	S	σ_t	σ_{stp}	ΣΔD	C	C_m	K
100	1576	3541	2614	2658	27.3	15119	15220	15
152	1427	3530	2638	2706	36.7	15080	15179	18
196	1352	3525	2650	2737	44.0	15061	15154	20
268	1251	3513	2661	2781	55.2	15037	15126	22
334	1165	3501	2668	2818	64.9	15017	15106	24
488	934	3473	2687	2907	86.1	14956	15068	22
726	738	3451	2700	3029	115.9	14917	15025	12
962	574	3441	2714	3152	143.0	14890	14995	-3
1210	372	3445	2740	3294	166.9	14849	14969	-25
1448	305	3452	2752	3415	185.7	14860	14950	-48
1688	270	3458	2760	3532	202.7	14885	14939	-69
1929	250	3460	2763	3642	219.0	14918	14934	-85
2402	208	3465	2771	3860	250.5	14979	14937	-101

D712

D	T	S	σ_t	σ_{stp}	ΣΔD	C	C_m	K
0	2228	3572	2471	2471	0.0	15290	15290	0
24	2150	3566	2488	2498	7.6	15272	15281	4
48	1852	3556	2559	2580	14.2	15195	15257	8
72	1671	3551	2599	2631	19.5	15144	15228	11
96	1603	3546	2611	2654	24.3	15128	15205	13
139	1511	3541	2628	2690	32.3	15105	15177	16
174	1445	3535	2638	2715	38.5	15089	15161	19
263	1306	3519	2655	2772	53.0	15056	15131	23
335	1204	3504	2663	2813	64.1	15031	15112	25
487	960	3472	2682	2902	85.8	14965	15076	25
718	719	3445	2698	3024	115.4	14907	15031	15
953	554	3439	2715	3149	142.4	14880	14997	-2
1199	410	3442	2734	3282	166.8	14861	14971	-23
1435	318	3450	2749	3406	186.6	14862	14953	-45
1672	277	3456	2758	3522	204.0	14886	14942	-65
1915	241	3460	2764	3638	220.6	14911	14936	-82
2391	219	3464	2769	3852	252.4	14982	14938	-99

D713

D	T	S	σ_t	σ_{stp}	ΣΔD	C	C_m	K
0	2229	3570	2469	2469	0.0	15290	15290	0
24	2224	3570	2470	2481	7.8	15292	15291	5
48	2211	3570	2474	2495	15.6	15293	15292	9
72	1757	3549	2577	2609	22.2	15169	15271	13
97	1591	3541	2610	2653	27.4	15123	15239	15
139	1441	3533	2637	2699	35.1	15081	15197	18
178	1375	3527	2647	2726	41.6	15066	15170	20
262	1264	3513	2658	2776	54.8	15041	15133	23
329	1183	3502	2666	2813	64.9	15023	15112	25
489	959	3472	2682	2903	87.5	14965	15073	24
710	749	3450	2698	3019	115.9	14918	15032	15
937	559	3439	2714	3141	142.1	14880	15000	-0
1178	416	3440	2731	3270	166.3	14860	14973	-21
1414	323	3448	2747	3394	186.5	14861	14954	-43
1890	244	3459	2763	3625	221.1	14909	14937	-80
2356	218	3462	2767	3836	252.7	14975	14938	-98

D714

D	T	S	σ_t	σ_{stp}	ΣΔD	C	C_m	K
0	2297	3573	2452	2452	0.0	15307	15307	0
28	2300	3579	2455	2467	9.5	15314	15310	6
56	2016	3570	2527	2552	18.1	15243	15294	11
85	1880	3567	2560	2598	25.6	15210	15271	15
106	1808	3563	2575	2622	30.5	15192	15257	18
158	1714	3559	2595	2665	41.9	15172	15233	24
209	1631	3553	2610	2703	52.4	15155	15216	30
275	1450	3535	2637	2759	64.7	15107	15195	36
346	1350	3522	2648	2802	76.8	15084	15175	40

D	T	S	σ_t	σ_{stp}	$\Sigma\Delta D$	C	C_m	K
D714 continued								
479	1056	3486	2676	2892	97.2	15000	15138	44
755	703	3447	2702	3044	133.0	14908	15070	35
970	564	3440	2715	3156	157.5	14887	15031	20
1230	407	3444	2736	3298	183.2	14867	14998	-1
1444	326	3450	2748	3409	201.1	14867	14979	-20
1626	292	3457	2757	3500	214.6	14885	14967	-35
1835	273	3460	2761	3598	229.2	14911	14959	-50
2216	236	3464	2768	3774	255.2	14960	14955	-66
D721								
0	2331	3572	2441	2441	0.0	15316	15316	0
26	2257	3574	2464	2475	8.9	15302	15309	5
52	2207	3572	2476	2499	17.3	15292	15303	11
78	1940	3563	2542	2576	24.9	15225	15288	15
104	1787	3561	2579	2625	31.2	15186	15267	19
147	1706	3559	2597	2662	40.5	15168	15241	24
203	1599	3548	2614	2704	51.8	15144	15217	29
249	1444	3534	2637	2748	60.3	15100	15200	33
278	1327	3521	2652	2776	65.1	15065	15187	35
444	1080	3490	2675	2875	90.1	15003	15130	38
750	702	3446	2701	3041	130.0	14907	15058	29
956	546	3435	2713	3148	153.6	14877	15022	14
1249	363	3445	2741	3313	181.8	14850	14985	-13
1472	297	3453	2753	3428	199.2	14860	14965	-35
1697	266	3457	2759	3535	215.0	14885	14953	-54
1962	243	3461	2765	3659	232.9	14920	14946	-71
2402	191	3466	2773	3863	261.2	14972	14946	-87
D722								
0	2380	3569	2424	2424	0.0	15327	15327	0
18	2380	3570	2425	2433	6.6	15331	15329	4
35	2332	3570	2439	2454	12.7	15322	15328	8
53	2289	3570	2452	2475	19.1	15313	15324	11
102	1924	3564	2547	2592	33.8	15224	15297	20
133	1838	3562	2567	2626	41.4	15206	15278	25
190	1721	3556	2591	2675	54.3	15179	15252	32
315	1470	3533	2631	2771	79.2	15119	15211	44
482	1145	3493	2666	2881	107.0	15033	15164	53
614	859	3458	2687	2965	125.7	14947	15126	52
757	708	3443	2698	3041	143.9	14909	15088	45
900	588	3436	2708	3118	160.8	14885	15058	35
D723								
0	2253	3574	2465	2465	0.0	15296	15296	0
26	2259	3577	2465	2477	8.5	15303	15300	5
52	2142	3571	2494	2517	16.8	15275	15294	10
78	1952	3564	2539	2574	24.2	15228	15280	15
104	1790	3561	2578	2624	30.5	15187	15262	18
153	1709	3556	2594	2662	41.2	15170	15235	24
262	1511	3443	2553	2669	66.7	15113	15196	34
D724								
0	2173	3569	2484	2484	0.0	15275	15275	0
19	2174	3571	2485	2493	5.9	15279	15277	4
38	2176	3571	2484	2501	11.8	15283	15279	7
57	2031	3560	2516	2541	17.5	15246	15274	10
77	1816	3553	2566	2600	22.7	15189	15259	13
109	1702	3553	2593	2642	29.9	15160	15234	17
130	1656	3553	2604	2662	34.2	15149	15221	19
184	1577	3550	2620	2702	44.7	15134	15198	24

D	T	S	σ_t	σ_{stp}	$\Sigma\Delta D$	C	C_m	K
D724 continued								
232	1475	3537	2633	2736	53.5	15109	15182	28
511	1015	3481	2680	2909	97.4	14990	15109	37
665	785	3455	2696	2997	117.6	14926	15074	33
985	332	3440	2740	3194	150.0	14794	15004	3
1158	393	3445	2738	3268	164.3	14848	14976	-18
1353	329	3453	2750	3370	179.9	14854	14958	-38
1545	285	3458	2759	3466	193.6	14869	14946	-56
1642	266	3466	2767	3518	199.9	14878	14942	-64
D726								
0	2191	3569	2479	2479	0.0	15280	15280	0
22	2193	3571	2480	2489	6.9	15284	15282	4
43	2193	3571	2480	2498	13.6	15287	15284	8
65	2001	3558	2522	2551	20.1	15240	15277	12
86	1694	3546	2590	2628	25.3	15154	15257	15
124	1494	3538	2630	2685	32.7	15097	15217	18
170	1398	3528	2643	2718	40.6	15072	15181	20
233	1318	3520	2653	2757	50.8	15055	15149	23
297	1257	3512	2659	2792	60.8	15044	15127	25
421	1082	3489	2674	2863	79.1	15001	15096	27
635	792	3455	2695	2983	107.5	14924	15051	21
839	630	3443	2709	3090	131.6	14893	15016	9
1057	485	3440	2724	3206	154.8	14869	14988	-8
1263	373	3444	2739	3317	173.9	14857	14967	-27
1469	305	3451	2751	3424	190.4	14863	14952	-47
1737	267	3456	2759	3552	209.8	14892	14941	-69
2006	234	3461	2765	3679	228.0	14924	14936	-85
D728								
0	2167	3573	2488	2488	0.0	15274	15274	0
26	2133	3568	2494	2505	7.9	15270	15272	5
53	2048	3567	2516	2540	15.8	15250	15266	9
79	1741	3553	2584	2619	22.3	15167	15247	13
106	1648	3550	2604	2651	28.0	15143	15223	16
155	1587	3545	2614	2683	37.7	15132	15196	20
214	1501	3538	2628	2723	48.7	15114	15176	25
284	1365	3524	2646	2773	60.9	15079	15156	30
349	1237	3507	2659	2815	71.3	15046	15139	32
500	1026	3482	2679	2903	93.4	14992	15102	34
786	717	3451	2703	3059	130.3	14919	15049	25
1505	326	3452	2750	3438	200.7	14879	14977	-23
1740	274	3458	2760	3554	217.9	14897	14965	-41
2070	231	3462	2766	3709	240.2	14933	14957	-60
D729								
0	2133	3564	2491	2491	0.0	15264	15264	0
24	2132	3565	2492	2502	7.3	15267	15266	4
51	2022	3557	2516	2538	15.2	15242	15260	9
79	1787	3549	2570	2605	22.5	15180	15242	13
106	1633	3546	2604	2651	28.3	15138	15221	16
157	1556	3542	2619	2689	38.2	15122	15191	20
202	1482	3536	2631	2721	46.5	15106	15174	23
251	1385	3528	2645	2757	54.9	15082	15158	27
325	1263	3513	2659	2804	66.8	15050	15137	30
479	1045	3486	2678	2894	89.4	14997	15101	32
647	775	3456	2699	2992	111.2	14919	15063	27
878	622	3446	2712	3111	137.9	14897	15022	13
1037	508	3445	2725	3198	154.5	14876	15001	1
1253	401	3448	2739	3312	174.4	14868	14979	-18
1383	367	3451	2745	3377	185.2	14875	14969	-29
1806	268	3459	2761	3585	217.0	14904	14950	-60

D730

D	T	S	σ_t	σ_{stp}	ΣΔD	C	C_m	K
0	2209	3581	2483	2483	0.0	15286	15286	0
34	2212	3579	2480	2495	10.7	15293	15289	7
53	2150	3579	2498	2521	16.5	15278	15288	10
119	1676	3553	2600	2652	33.2	15154	15248	20
186	1630	3550	2608	2690	46.8	15151	15213	26
250	1489	3539	2631	2743	59.0	15117	15193	32
318	1384	3528	2646	2787	70.7	15091	15174	37
396	1273	3513	2657	2833	83.5	15065	15155	41
573	1008	3482	2682	2939	109.7	14999	15117	45
712	820	3450	2687	3009	128.5	14947	15088	42
887	732	3443	2695	3095	151.5	14941	15060	35
1344	378	3447	2741	3355	200.5	14873	15007	7
1520	319	3455	2753	3448	214.5	15878	14992	-8

D731

D	T	S	σ_t	σ_{stp}	ΣΔD	C	C_m	K
0	2200	3580	2484	2484	0.0	15284	15284	0
22	2203	3581	2484	2494	6.8	15288	15286	4
43	2204	3582	2485	2504	13.4	15291	15287	8
65	2194	3581	2487	2515	20.2	15293	15289	13
86	2007	3569	2529	2567	26.4	15246	15284	16
108	1777	3562	2582	2630	31.8	15183	15270	19
131	1718	3558	2593	2651	36.8	15169	15253	22
192	1631	3553	2710	2695	49.3	15153	15224	29
252	1551	3545	2622	2734	60.9	15137	15205	34
358	1377	3527	2646	2805	79.8	15097	15179	43
578	1060	3489	2678	2937	113.8	15018	15132	51
798	759	3455	2700	3061	142.9	14937	15089	48
1030	571	3441	2714	3182	169.8	14900	15051	35
1250	414	3444	2735	3306	191.9	14873	15021	18
1470	312	3457	2755	3428	209.6	14867	14999	-1
1685	276	3460	2761	3531	224.5	14888	14983	-19
2063	228	3465	2769	3709	249.1	14932	14970	-42

D733

D	T	S	σ_t	σ_{stp}	ΣΔD	C	C_m	K
0	2360	3559	2423	2423	0.0	15321	15321	0
22	2359	3560	2424	2433	8.1	15324	15323	5
44	2363	3559	2422	2441	16.3	15330	15325	10
66	2062	3569	2514	2543	23.5	15257	15315	14
88	1951	3567	2542	2581	29.5	15230	15297	17
124	1875	3566	2561	2615	38.6	15215	15275	23
194	1751	3560	2587	2673	54.8	15190	15249	32
245	1663	3553	2603	2711	65.7	15171	15234	38
323	1479	3536	2631	2775	80.8	15124	15213	46
651	877	3469	2693	2987	131.4	14960	15127	55
840	705	3445	2700	3080	155.0	14923	15085	47
996	594	3443	2713	3165	173.3	14904	15057	38
1193	441	3445	2733	3277	193.3	14874	15029	23
1505	321	3455	2753	3441	219.3	14877	14997	-3

D734

D	T	S	σ_t	σ_{stp}	ΣΔD	C	C_m	K
0	2351	3560	2426	2426	0.0	15319	15319	0
21	2335	3562	2432	2441	7.6	15319	15319	4
46	2221	3573	2473	2493	16.2	15296	15313	10
70	1999	3567	2529	2560	23.3	15240	14297	14
95	1796	3560	2576	2618	29.6	15187	15275	17
155	1653	3551	2603	2672	42.5	15153	15234	24
202	1575	3546	2618	2707	51.7	15137	15213	29
264	1452	3536	2637	2755	63.1	15106	15192	34
332	1327	3522	2653	2801	74.4	15075	15171	38
481	1069	3489	2676	2892	96.9	15006	15130	42
730	746	3455	2702	3033	129.2	14923	15073	36

D734 continued

D	T	S	σ_t	σ_{stp}	ΣΔD	C	C_m	K
932	564	3448	2721	3145	151.5	14882	15036	22
1158	444	3448	2735	3264	173.2	14870	15004	3
1424	346	3454	2750	3401	195.4	14873	14979	-20
1620	293	3459	2759	3499	209.7	14884	14967	-36
1850	264	3462	2764	3607	225.3	14911	14958	-52
2362	214	3465	2770	3841	259.2	14975	14955	-71

D735

D	T	S	σ_t	σ_{stp}	ΣΔD	C	C_m	K
0	2350	3565	2430	2430	0.0	15319	15319	0
24	2334	3566	2436	2446	8.6	15319	15319	5
47	2219	3566	2469	2489	16.5	15295	15313	10
71	1998	3554	2520	2551	23.8	15238	15297	14
95	1798	3548	2566	2608	30.0	15186	15276	17
140	1653	3542	2597	2659	40.1	15149	15241	22
190	1575	3535	2609	2693	50.3	15132	15214	27
270	1452	3525	2629	2749	65.5	15106	15186	33
332	1327	3515	2647	2795	76.3	15074	15168	37
479	1070	3496	2682	2897	98.5	15007	15129	41
729	746	3469	2713	3043	129.0	14923	15072	35
932	564	3454	2726	3150	149.9	14882	15035	22
1160	443	3443	2731	3261	171.6	14869	15003	2
1424	346	3443	2741	3392	195.2	14872	14978	-21
1622	293	3447	2749	3490	211.4	14884	14966	-37
1851	264	3454	2757	3601	228.8	14910	14957	-53
2362	214	3462	2768	3839	264.8	14975	14954	-72

D736

D	T	S	σ_t	σ_{stp}	ΣΔD	C	C_m	K
0	2267	3569	2457	2457	0.0	15299	15299	0
24	2235	3572	2469	2479	7.9	15295	15297	5
49	2204	3572	2477	2499	16.0	15292	15295	10
73	2057	3564	2512	2544	23.3	15255	15288	14
98	1847	3559	2562	2606	29.9	15201	15273	18
133	1707	3555	2594	2653	37.9	15167	15249	22
152	1638	3548	2605	2672	41.8	15148	15238	24
234	1505	3538	2627	2731	57.6	15118	15201	31
288	1418	3530	2640	2768	67.1	15098	15183	35
407	1201	3505	2664	2847	86.4	15043	15150	41
633	849	3464	2694	2980	117.7	14947	15094	40
807	691	3450	2706	3072	138.7	14912	15058	31
1049	553	3444	2719	3196	165.5	14896	15022	16
1243	428	3443	2733	3300	184.8	14877	15001	1
1436	354	3449	2745	3401	201.7	14879	14984	-15
1664	309	3456	2755	3514	219.5	14898	14971	-32
2088	241	3467	2770	3719	248.7	14941	14961	-55

D737

D	T	S	σ_t	σ_{stp}	ΣΔD	C	C_m	K
0	2316	3564	2439	2439	0.0	15311	15311	0
22	2301	3564	2444	2453	7.7	15310	15311	5
44	2155	3573	2492	2511	14.9	15279	15303	9
66	1955	3562	2537	2566	21.2	15227	15286	13
88	1817	3560	2571	2610	26.7	15191	15267	16
132	1688	3554	2597	2656	36.4	15161	15236	21
175	1619	3549	2610	2687	45.1	15146	15216	25
239	1500	3543	2632	2738	57.1	15117	15193	31
306	1372	3525	2646	2782	68.7	15085	15173	35
426	1148	3500	2671	2861	87.4	15027	15140	40
643	856	3464	2693	2983	117.0	14951	15089	38
842	680	3450	2707	3089	141.1	14914	15051	29
1062	540	3449	2725	3208	164.8	14893	15021	15
1271	432	3451	2738	3318	184.5	14884	14999	-1
1478	350	3455	2750	3425	201.6	14885	14983	-17

D	T	S	σ_t	σ_{stp}	ΣΔD	C	C_m	K
D737 continued								
1689	294	3459	2759	3529	217.2	14896	14971	-33
2136	232	3463	2767	3738	247.7	14945	14960	-56
D738								
0	2242	3568	2464	2464	0.0	15293	15293	0
22	2206	3572	2477	2486	7.1	15287	15290	4
45	2204	3574	2479	2498	14.5	15292	15290	9
67	2032	3567	2521	2550	21.0	15249	15283	13
90	1902	3560	2549	2589	27.1	15216	15270	16
135	1738	3555	2586	2646	37.8	15176	15245	22
180	1642	3548	2604	2683	47.3	15153	15225	27
239	1534	3543	2625	2731	58.8	15128	15204	33
305	1422	3529	2638	2774	70.6	15102	15185	38
431	1144	3500	2671	2864	90.7	15025	15149	43
644	920	3475	2691	2981	119.9	14977	15100	43
854	739	3459	2706	3092	145.9	14940	15065	37
1087	562	3450	2723	3216	171.6	14907	15034	25
1309	434	3450	2737	3334	192.9	14892	15011	10
1538	343	3455	2751	3452	212.1	14892	14993	-7
1759	289	3460	2760	3562	228.4	14907	14981	-22
2054	242	3463	2766	3701	248.5	14936	14973	-37